July–December 2025 Volume 33 Issue 2 ISSN 0970-1842

JAS Journal of Anatomical Sciences

UP Chapter of the Anatomical Society of India

JAS

Also available online at
www.jaypeejournals.com
www.asiupjas.com

Editor-in-Chief
Satyam Khare

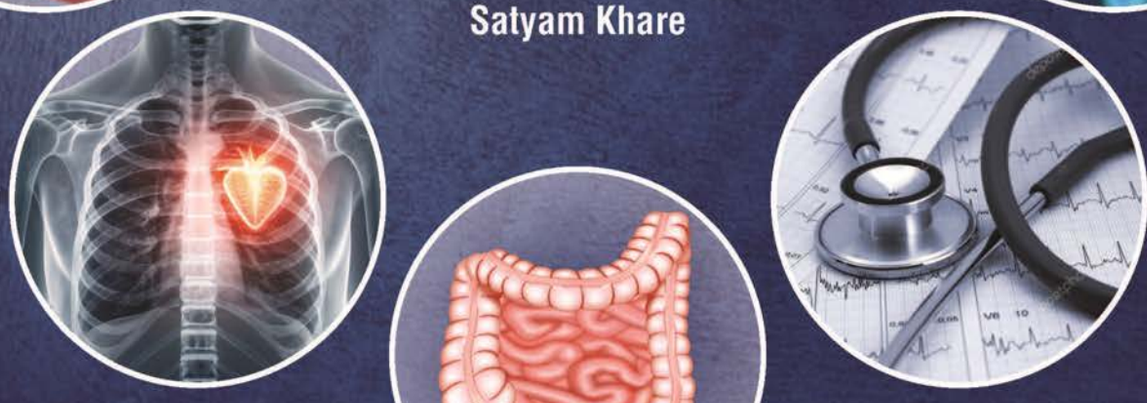

JAYPEE Jaypee Journals

SDG PUBLISHERS COMPACT

July–December 2025 Volume 33 Issue 2
Journal of Anatomical Sciences
ISSN 0970-1842

EDITORIAL

Aligning Anatomy Teaching with Competency-based Medical Education: Reflections and Future Directions

Satyam Khare

Keywords: Anatomy education, Assessment methods, Competency-based medical education, Early clinical exposure.
Journal of Anatomical Sciences (2025): 10.5005/jas-11049-0015

Department of Anatomy, Subharti Medical College, Swami Vivekanand Subharti University, Meerut, Uttar Pradesh, India

Corresponding Author: Satyam Khare, Department of Anatomy, Subharti Medical College, Swami Vivekanand Subharti University, Meerut, Uttar Pradesh, India, Phone: +91 9837083748, e-mail: satyamkhare@subharti.co

How to cite this article: Khare S. Aligning Anatomy Teaching with Competency-based Medical Education: Reflections and Future Directions. J Anat Sciences 2025;33(2):31–32.

Source of support: Nil

Conflict of interest: None

The introduction of competency-based medical education (CBME) by the National Medical Commission has, over the past few years, unsettled many long-held assumptions about how anatomy should be taught, learned, and assessed. For a discipline that has traditionally been anchored in structure, sequence, and a certain reverence for detail, the shift toward competencies and outcomes has not always felt intuitive. Yet, as implementation matures, it is becoming increasingly clear that anatomy is neither peripheral nor resistant to CBME; rather, it sits at its very core.

Anatomy has long been the first sustained encounter medical students have with the human body. Dissection halls, osteology rooms, and histology labs have historically shaped professional identity as much as cognitive knowledge. Competency-based medical education asks us to reconsider whether this early exposure translates into demonstrable abilities later in clinical practice. That question, uncomfortable as it may be, is not entirely misplaced. Knowing the branches of an artery is one thing; applying that knowledge safely during a procedure, or explaining its relevance to a patient, is quite another.

The Graduate Medical Education Regulations emphasize the production of an Indian Medical Graduate who is competent, ethical, and responsive to societal needs.[1] Anatomy, in this framework, is expected to contribute not merely factual knowledge but observable competencies—ranging from basic procedural skills to professional attitudes. Early clinical exposure, vertical integration, and attitude, ethics and communication (AETCOM) modules have nudged anatomy departments into spaces that were earlier considered outside their traditional remit.[2] Some faculty have embraced this shift readily; others remain cautious, perhaps rightly so.

One area where hesitation often surfaces is assessment. Anatomy assessments have historically rewarded recall and spatial understanding, frequently through written examinations and spotters. Competency-based medical education encourages workplace-based assessment tools, formative feedback, and longitudinal observation.[3] Translating these ideas into the anatomy curriculum is not straightforward. While objective structured practical examinations (OSPEs) appear to fit neatly into the CBME vocabulary, their execution sometimes risks becoming a cosmetic change rather than a conceptual one. When an OSPE station tests labeling rather than application, the underlying philosophy remains unchanged.

There is also the question of time. Anatomy teaching hours have been rationalized across many curricula, sometimes leading to a perception of loss. Faculty often express concern that reduced dissection time may erode foundational understanding. That concern may not be entirely unfounded. At the same time, evidence suggests that focused, clinically contextualized anatomy teaching may achieve comparable learning outcomes, particularly when reinforced across phases.[4] What seems to matter more than sheer duration is how and where anatomical knowledge is revisited.

Technology has entered this conversation almost by default. Virtual dissection tables, three-dimensional software, and online modules are frequently presented as solutions aligned with CBME. They certainly offer flexibility and visualization advantages, especially in large classes. Still, it may be worth acknowledging that technology is a means rather than an end. Without thoughtful integration, digital tools risk becoming parallel curricula that students engage with superficially. Many teachers have quietly noted that a brief discussion around a cadaveric variation often leaves a deeper impression than an impeccably rendered digital model.

Faculty development remains another uneven terrain. Competency-based medical education expects anatomy teachers to function as facilitators, assessors, and mentors, roles for which many were not formally trained. Workshops and orientation programs have attempted to bridge this gap, but their impact appears variable.[5] Some changes are absorbed easily; others take time, repetition, and peer discussion. Informal conversations in faculty rooms often reveal a gradual shift in thinking, even among those initially skeptical of CBME.

From the student's perspective, the transition has been equally complex. First-year students now encounter anatomy alongside communication skills, ethics, and early patient interactions. While this integration is conceptually sound, it can feel fragmented in practice. Students sometimes struggle to see how surface anatomy sessions connect with bedside encounters, especially when clinical

exposure is observational rather than participatory. This gap may narrow as departments collaborate more closely, but it underscores the need for coherence rather than mere coexistence of curricular elements.[6]

One cannot ignore the broader institutional context. Medical colleges vary widely in infrastructure, faculty strength, and patient load. Competency-based medical education allows for flexibility, but implementation inevitably reflects local realities. Anatomy departments in resource-constrained settings may adopt different strategies from those in well-equipped institutions, and that diversity should not automatically be viewed as deviation. What matters is alignment with core competencies rather than uniformity of methods.

Looking ahead, anatomy education under CBME is likely to become more longitudinal, less siloed, and increasingly reflective. There may be greater emphasis on clinical anatomy taught closer to the point of care, with preclinical foundations revisited rather than front-loaded. Assessment may gradually shift toward integrated formats where anatomy knowledge is inferred through clinical reasoning rather than directly tested. These changes will not occur uniformly or without friction, but incremental adaptation seems more realistic than radical overhaul.[7]

As anatomists, there is perhaps a need to let go of the idea that rigor is synonymous with volume. Rigor, in a competency-based framework, lies in relevance, consistency, and the ability to justify why a particular piece of knowledge matters. Anatomy has survived many curricular reforms over the decades. It is likely to adapt to this one as well, not by abandoning its identity, but by articulating its value in the language of competence and care.

If CBME asks uncomfortable questions of anatomy, it also offers an opportunity. It invites us to reflect on what we truly want our students to carry forward from the first year into lifelong practice. The answers may not always be tidy, but they are worth pursuing.

References

1. National Medical Commission. Graduate Medical Education Regulations, 2019. New Delhi: NMC; 2019.
2. National Medical Commission. Competency Based Undergraduate Curriculum for the Indian Medical Graduate, Volume I. New Delhi: NMC; 2020.
3. Frank JR, Snell LS, Cate OT, et al. Competency-based medical education: Theory to practice. Med Teach 2010;32(8):638–645. DOI: 10.3109/0142159X.2010.501190.
4. Bergman EM, de Bruin ABH, Herrler A, et al. Students' perceptions of anatomy across the undergraduate problem-based learning medical curriculum: A phenomenographical study. BMC Med Educ 2013;13:152. Published 2013 Nov 19. DOI: 10.1186/1472-6920-13-152.
5. Modi JN, Gupta P, Singh T. Competency-based medical education, entrustment and assessment. Indian Pediatr 2015;52(5):413–420. DOI: 10.1007/s13312-015-0647-5.
6. Harden RM. Outcome-based education: The future is today. Med Teach 2007;29(7):625–629. DOI: 10.1080/01421590701729930.
7. Drake RL, McBride JM, Lachman N, et al. Medical education in the anatomical sciences: The winds of change continue to blow. Anat Sci Educ 2009;2(6):253–259. DOI: 10.1002/ase.117.

ORIGINAL RESEARCH

Morphometric Analysis of the L4–L5 Lumbar Intervertebral Foramen in Adults: A Computed Tomography-based Observational Study

Balamurali M Nair [1], Mahendra Kathole[2], Vandana Mehta[3], Mahesh K Mittal[4]

Received on: 10 October 2025; *Accepted on*: 04 November 2025; *Published on*: 20 January 2026

Abstract

Introduction: The lumbar intervertebral foramen (IVF) serves as a passage for spinal nerves and vessels, and its dimensions may vary with age and sex. Morphometric data derived from imaging can enhance understanding of foraminal anatomy and its clinical implications. The present study aimed to analyze the morphometry of the L4–L5 IVF using computed tomography (CT) and to evaluate age- and sex-related differences in selected parameters.

Materials and methods: This observational, cross-sectional study included 51 asymptomatic adult CT scans (25 males, 26 females; mean age 35.82 ± 12.61 years) obtained in the supine position. Sagittal images at the exit slice of the L4–L5 IVF were analyzed using RadiAnt DICOM Viewer. Four parameters were measured: Disc height (DH), pedicle to superior articular process distance (P-SAP), posteroinferior margin of the upper vertebra to superior articular process distance (IPV-SAP), and pedicle to inferior vertebra distance (P-IV). Data were analyzed using SPSS v22. Statistical tests included *t*-test, Wilcoxon–Mann–Whitney *U*-test, and Spearman correlation, with significance set at $p < 0.05$.

Results: Males showed greater DH and P-SAP values bilaterally compared with females, whereas IPV-SAP and P-IV values exhibited minor sex differences. The IPV-SAP distance at the exit slice was significantly higher in individuals aged >40 years, suggesting age-related morphological widening of the foramen. Other parameters showed nonsignificant but similar trends.

Conclusion: The exit zone of the L4–L5 IVF exhibits subtle age-related dimensional changes, particularly in the IPV-SAP distance, which may reflect adaptive or degenerative alterations. These morphometric findings provide valuable baseline data for anatomical and radiological reference and may aid in the interpretation of age-related lumbar foraminal narrowing.

Keywords: Age-related changes, Anatomy, Computed tomography, Intervertebral foramen, Lumbar spine, Morphometry.

Journal of Anatomical Sciences (2025): 10.5005/jas-11049-0009

Introduction

The lumbar intervertebral foramen (IVF) serves as a critical passageway for the spinal nerve roots, dorsal root ganglia, and accompanying vessels.[1] Anatomical variations in the dimensions of the lumbar IVF can influence nerve root mobility and susceptibility to compression, contributing to clinical conditions such as radiculopathy and lumbar spinal stenosis.[2–4] The L4–L5 level is particularly significant, as it represents the most mobile segment of the lumbar spine and is a common site of degenerative changes affecting the exiting nerve root.[5]

Morphometric evaluation of the lumbar IVF provides essential baseline data for anatomical education, radiological interpretation, and surgical planning, particularly for procedures involving transforaminal approaches or pedicle screw placement. Previous studies have primarily utilized cadaveric specimens or magnetic resonance imaging (MRI) imaging to assess foraminal dimensions, revealing variations associated with sex, side, and age.[6–9] However, computed tomography (CT)-based morphometric studies offer precise bony measurements and facilitate accurate assessment of foraminal geometry in living subjects.

Despite its clinical and anatomical relevance, limited CT-based data exist on normative dimensions of the L4–L5 IVF in adult populations.[10] Establishing such reference values is critical for distinguishing normal anatomical variability from pathological narrowing or degenerative changes. Moreover, age- and sex-related variations may have implications for spinal biomechanics and surgical decision-making.

Therefore, the present study aims to perform a CT-based morphometric analysis of the L4–L5 lumbar IVF in adults, evaluating parameters including disc height (DH), pedicle to superior articular process distance (P-SAP), posteroinferior margin to superior articular process distance (IPV-SAP), and pedicle to inferior vertebra distance (P-IV).[11] The study further investigates variations according to sex,

[1–3]Department of Anatomy, Vardhman Mahavir Medical College and Safdarjung Hospital, New Delhi, India

[4]Department of Radiology, Vardhman Mahavir Medical College and Safdarjung Hospital, New Delhi, India

Corresponding Author: Balamurali M Nair, Department of Anatomy, Vardhman Mahavir Medical College and Safdarjung Hospital, New Delhi, India, Phone: +91 7012976315, e-mail: balamurali.m1@gmail.com

How to cite this article: Nair BM, Kathole M, Mehta V, *et al*. Morphometric Analysis of the L4–L5 Lumbar Intervertebral Foramen in Adults: A Computed Tomography-based Observational Study. J Anat Sciences 2025;33(2):33–37.

Source of support: Nil

Conflict of interest: None

side, and age-group, providing normative anatomical data for clinical and educational reference.

Materials and Methods

Study Design and Setting

This observational, cross-sectional study was conducted in the Department of Anatomy in collaboration with the Department of Radiology, Vardhman Mahavir Medical College and Safdarjung Hospital, New Delhi, over a period of 18 months. Ethical clearance was obtained from the Institutional Ethics Committee and Institutional Review Board prior to data collection.

Sample Size and Participants

The sample size was determined based on a previous study by Yan et al., which reported a standard deviation of 3.64 mm in foraminal measurements. At a 95% confidence interval and absolute error of 1 mm, the calculated sample size was 51 using the formula:

$$n = \frac{Z_{\alpha}^2 \sigma^2}{E^2} = \frac{(1.96)^2 (3.64)^2}{1^2} = 50.9$$

Thus, 51 adult CT scans were included in the study. Participants were divided into two age-groups: ≤40 years ($n = 36$) and >40 years ($n = 15$). The sample comprised 25 males and 26 females, with a mean age of 35.82 ± 12.61 years.

Inclusion and Exclusion Criteria

Inclusion criteria included CT scans of adults (≥18 years) with complete lumbar segments and no radiological artifacts.

Exclusion criteria were scans showing evidence of current or previous back pain, congenital spinal anomalies, traumatic deformities, or degenerative spinal disease.

CT Data Acquisition

High-resolution CT images of the lumbar spine were obtained in the supine position using a multi-detector CT scanner in the Department of Radiology. Images were reconstructed in sagittal and axial planes and exported in digital imaging and communications in medicine (DICOM) format for analysis.

Image Analysis and Measurement Protocol

All measurements were performed using RadiAnt DICOM Viewer (Medixant, Poland). For consistency, analysis focused on the exit slice of the L4–L5 IVF, defined as the sagittal slice showing the last closed bony boundary of the foramen before the nerve root exits laterally (Fig. 1).

Parameters Measured

- Disc height: Distance between the posteroinferior edge of the upper vertebra and posterosuperior edge of the lower vertebra (Fig. 2).
- Pedicle to superior articular process distance: From the top of the superior articular process of the lower vertebra to the inferior aspect of the upper vertebra pedicle (Fig. 3).
- Posteroinferior margin to superior articular process distance: From the posteroinferior margin of the upper vertebra to the superior articular process of the vertebra below (Fig. 4).
- Pedicle to inferior vertebra distance: From the inferior border of the upper pedicle to the inferior border of the same vertebra, measured perpendicularly (Fig. 5).

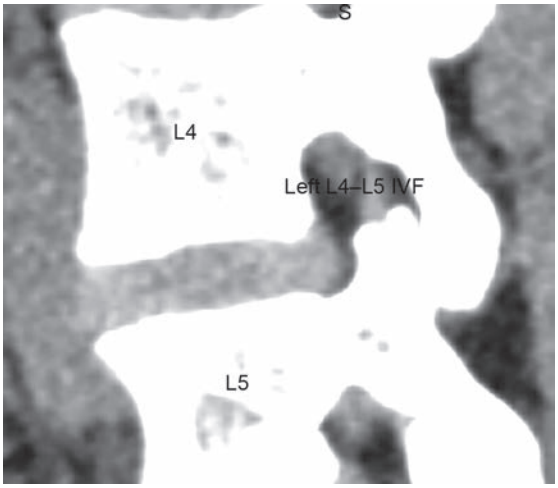

Fig. 1: Showing the exit slice of the left lumbar IVF at the L4–L5 level of a 44-year-old male

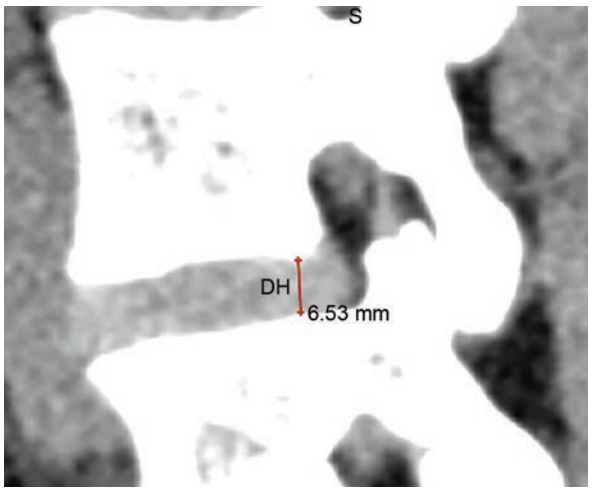

Fig. 2: Showing the measurement of DH at the L4–L5 level

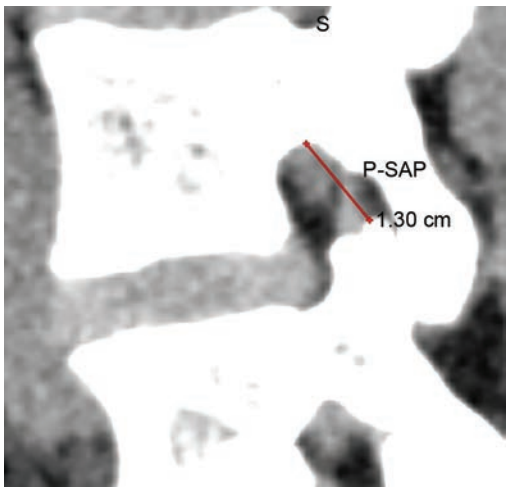

Fig. 3: Showing the measurement of pedicle to superior articular process distance (P-SAP) at the L4–L5 level

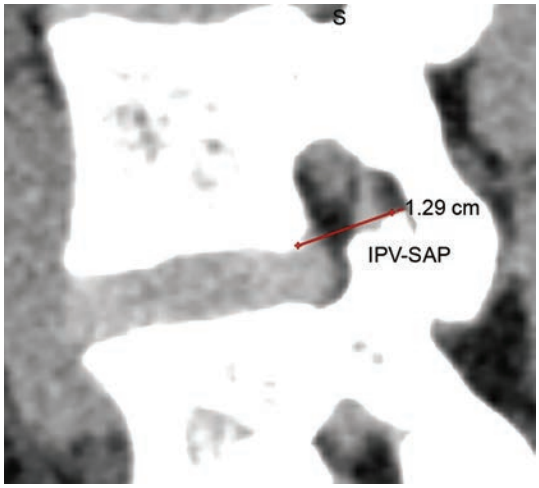

Fig. 4: Showing the measurement of IPV-SAP at the L4–L5 level

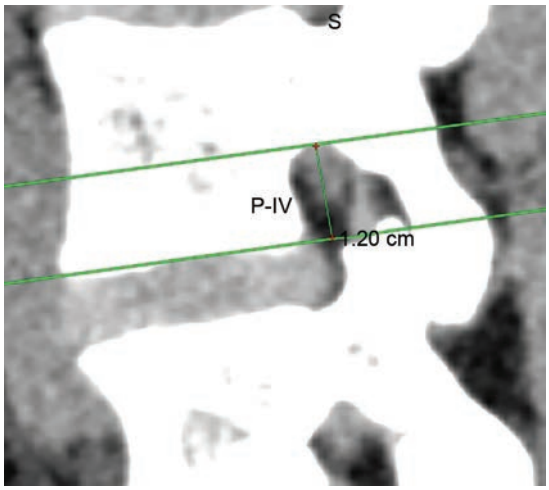

Fig. 5: Showing the measurement of P-IV at the L4–L5 level

Statistical Analysis

Measurements were analyzed using SPSS version 22. Parametric data were compared using *t*-test; nonparametric data were analyzed with Wilcoxon–Mann–Whitney *U*-test, paired Wilcoxon, and Friedman tests. Age distribution was tested with Shapiro–Wilk, and correlations were assessed using Spearman's coefficient. A p-value < 0.05 was considered statistically significant. Sex- and age-based comparisons were performed to assess anatomical variations.

Results

The present study included 51 subjects with a mean age of 35.82 ± 12.61 years (36 subjects ≤40 years, 15 subjects >40 years). There were 25 males and 26 females (Table 1).

Disc height at the L4–L5 exit slice showed values, with males exhibiting significantly greater DH (right: 6.61 ± 0.92 mm, left: 6.60 ± 0.97 mm) than females (right: 4.99 ± 1.60 mm, left: 5.16 ± 1.77 mm) ($p < 0.001$) (Tables 2 to 5).

Pedicle to superior articular process distance demonstrated L4–L5 exit slice means of approximately 11.39 ± 2.01 mm (right) and 11.24 ± 2.08 mm (left). Males had significantly larger P-SAP values at the L4–L5 exit slice than females ($p < 0.001$) (Tables 2 to 5).

Table 1: Age/gender summary

Age/gender	*Frequency (%)*	*Mean ± SD/median (IQR)*	*Min–Max*
Age (years)	–	35.82 ± 12.61/35.00 (26.00–42.50)	19–75
≤40 years	36 (70.6%)	–	–
>40 years	15 (29.4%)	–	–
Male	25 (49%)	–	–
Female	26 (51%)	–	–

Table 2: Showing the mean values of parameters at the L4–L5 level

Parameter	*Exit slice (mean ± SD)*
DH	5.83 ± 1.56
P-SAP	11.32 ± 2.04
IPV-SAP	10.43 ± 1.82
P-IV	9.8 ± 1.34

Table 3: Showing the mean values of parameters at the L4–L5 level with the right and left sides separately

Parameter	*Right (mean ± SD)*	*Left (mean ± SD)*
DH	5.79 ± 1.53	5.79 ± 1.53
P-SAP	11.39 ± 2.01	11.24 ± 2.08
IPV-SAP	10.54 ± 1.89	10.33 ± 1.77
P-IV	9.74 ± 1.31	9.85 ± 1.38

Posteroinferior margin of upper vertebra to superior articular process distance with L4–L5 exit slice means of 10.54 ± 1.89 mm (right) and 10.33 ± 1.77 mm (left). Posteroinferior margin to superior articular process distance values were generally higher in females (Tables 2 to 5).

Pedicle to inferior vertebra distance decreased from the entrance to exit slice at L4–L5, with exit slice means around 9.74 ± 1.31 mm (right) and 9.85 ± 1.38 mm (left). No significant gender differences were observed for P-IV at the exit slice (Tables 2 to 5).

Age-related correlations revealed significant negative associations between P-SAP at exit slices and age at the L4–L5 level, indicating potential foraminal narrowing with advancing age. Posteroinferior margin to superior articular process distance and DH showed variable associations with age, but were not statistically significant at the L4–L5 exit slice.

Discussion

Overview of Findings

The present CT-based morphometric study of the L4–L5 IVF establishes normative quantitative data for the adult Indian population. Among the four parameters analyzed (DH, P-SAP, IPV-SAP, and P-IV), males exhibited higher mean values than females, though most differences were not statistically significant. A significant increase in IPV-SAP was observed in participants older than 40, suggesting an age-related widening of the exit zone. Other parameters showed similar nonsignificant increasing trends.

Comparison with Previous Studies

Few anatomical studies have quantitatively examined the L4–L5 foramen using CT imaging.

Table 4: Showing the mean values of parameters in two age-groups at the L4–L5 level

	Right			*Left*		
Parameter	*≤40 years (mean ± SD)*	*>40 years (mean ± SD)*	*p-value*	*≤40 years (mean ± SD)*	*>40 years (mean ± SD)*	*p-value*
DH	5.68 ± 1.75	6.04 ± 0.83	0.687	5.82 ± 1.80	6.00 ± 0.97	0.959
P-SAP	11.24 ± 1.84	11.75 ± 2.42	0.796	11.23 ± 1.91	11.25 ± 2.51	0.926
IPV-SAP	10.13 ± 2.05	11.52 ± 0.87	0.02	9.88 ± 1.86	11.42 ± 0.87	0.008
P-IV	9.70 ± 0.88	9.82 ± 2.05	0.679	9.79 ± 0.88	10.00 ± 2.20	0.649

Table 5: Showing the mean values of parameters in both the gender at the L4–L5 level

	Right			*Left*		
Parameter	*Male (mean ± SD)*	*Female (mean ± SD)*	*p-value*	*Male (mean ± SD)*	*Female (mean ± SD)*	*p-value*
DH	6.61 ± 0.92	4.99 ± 1.60	<0.001	6.60 ± 0.97	5.16 ± 1.77	0.001
P-SAP	12.24 ± 1.69	10.58 ± 1.99	0.01	12.13 ± 1.73	10.38 ± 2.04	0.025
IPV-SAP	10.27 ± 1.43	10.80 ± 2.24	0.274	10.07 ± 1.48	10.58 ± 2.00	0.401
P-IV	9.81 ± 1.62	9.66 ± 0.96	0.828	9.86 ± 1.76	9.85 ± 0.91	0.497

Table 6: Comparison of values with previous study

	Yan et al.		*Present study*	
Parameter	*≤40 years*	*>40 years*	*≤40 years*	*>40 years*
DH	5.60 ± 1.17	6.11 ± 1.07	6.73 ± 1.08	6.43 ± 0.61
P-SAP	11.75 ± 1.60	12.23 ± 1.93	11.92 ± 1.14	12.72 ± 2.28
IPV-SAP	10.71 ± 2.25	10.73 ± 2.66	9.51 ± 1.12	11.41 ± 1.05

- Disc height: The present mean DH values (≈6.6 mm in males, ≈5.1 mm in females) correspond well with earlier morphometric data obtained from cadaveric and MRI studies, which reported DH ranging from 5 to 7 mm in asymptomatic adults.[12–14] Similar to Yan et al.,[11] our study also showed that DH at the exit slices decreased with age (Table 6).
- Pedicle-related parameters (P-SAP and P-IV): The current findings align with those of Bulyshchenko et al.,[10] who demonstrated slightly larger foraminal dimensions in males, attributable to generally larger vertebral body size and pedicle width. Studies by Senoo et al.,[6] Gkasdaris et al.,[15] and Al-Hadidi et al.,[16] showed a decrease in foraminal height with age, which aligns with the present study.
- Posteroinferior margin to superior articular process distance: The observed increase in IPV-SAP with advancing age differs from the gradual foraminal narrowing often described in degenerative changes.[6] This variation may represent compensatory remodeling of the posterior elements or individual anatomical adaptation rather than actual stenotic alteration.

Anatomical and Functional Implications

The L4–L5 IVF represents the passageway for the L4 spinal nerve root and accompanying vessels.[1] Its dimensions are influenced by DH, facet joint orientation, and pedicle morphology.

An increased IPV-SAP distance in older adults may indicate a relative superior shift of the superior articular process or mild facet degeneration, altering the posterior boundary of the foramen. Although this increase does not necessarily suggest reduced nerve compression risk, it highlights the dynamic geometry of the foramen across age-groups.[11,17]

Understanding these relationships is crucial for radiologists and spine surgeons when interpreting foraminal dimensions in CT or MRI images, particularly in differentiating physiological variations from pathological narrowing.

Sex- and Side-related Observations

The slightly larger foraminal dimensions in males observed here are consistent with general skeletal dimorphism.[18] The absence of significant laterality implies symmetrical development of lumbar foramina in the normal population, confirming that side-to-side variations on imaging are more likely pathological or postural in nature rather than inherent anatomical differences.

Clinical Relevance

Morphometric data from the present study provide baseline reference values for the L4–L5 IVF.[19] These measurements can assist in:

- Radiological evaluation of lumbar radiculopathy by distinguishing normal anatomical limits from true foraminal stenosis.
- Preoperative planning for transforaminal approaches, pedicle screw placement, and other spinal procedures.
- Educational and anthropometric purposes, supporting anatomical variability data across populations.

Limitations

While offering excellent bony detail, the use of CT lacks assessment of soft-tissue components such as ligaments and nerve roots. Future studies integrating MRI correlation, three-dimensional (3D) reconstruction, and larger multi-ethnic samples could further elucidate age-related and degenerative changes in foraminal morphology.

Conclusion

The present morphometric analysis of the lumbar IVF using CT at the L4–L5 level provides detailed quantitative insight into age-related variations, particularly at the exit zone where the nerve root transitions to the extraforaminal space. Among the evaluated parameters, the IPV-SAP demonstrated a statistically significant increase in individuals over 40 years, suggesting a tendency toward posterior widening of the foramen exit with advancing age. Although other parameters, such as P-SAP and DH, exhibited similar trends, they did not reach statistical significance, indicating

that the morphological adaptation may be localized or subtle in nature at this level.

These findings imply that the geometric characteristics of the L4–L5 IVF are not static but undergo measurable changes through adulthood. The widening of IPV-SAP with age could reflect remodeling associated with facet joint orientation, disc degeneration, or alterations in spinal curvature, which collectively modify the three-dimensional spatial relationships of foraminal boundaries. The stability of other parameters suggests that bony dimensions remain relatively preserved even when degenerative changes occur, underscoring the complexity of foraminal dynamics.

Overall, this study contributes to the anatomical understanding of the lumbar IVF by providing age-specific morphometric data derived from CT-based assessment. These results may serve as a reference for future investigations on lumbar nerve root compression syndromes, degenerative spinal disorders, and age-related morphological remodeling of the lumbar spine. Further large-scale studies integrating three-dimensional reconstruction and dynamic imaging could elucidate the functional implications of these anatomical changes.

Orcid

Balamurali M Nair https://orcid.org/0009-0002-9780-9270
Mahendra Kathole https://orcid.org/0009-0003-5536-5648
Vandana Mehta https://orcid.org/0000-0001-7386-9696

References

1. Amonoo-Kuofi HS, El-Badawi MG, Fatani JA. Ligaments associated with lumbar intervertebral foramina. J Anat 1988;156:177–183. PMCID: PMC1261921.
2. Edelson JG, Nathan H. Nerve root compression in spondylolysis and spondylolisthesis. J Bone Joint Surg – Ser B 1986;68(4):596–599. DOI: 10.1302/0301-620X.68B4.3733837.
3. Spivak JM, Kummer FJ, Chen D, et al. Intervertebral foramen size and volume changes in low grade, low dysplasia isthmic spondylolisthesis. Spine (Phila Pa 1976) 2010;35(20):1829–1835. DOI: 10.1097/BRS.0b013e3181eaa332.
4. Kaneko Y, Matsumoto M, Takaishi H, et al. Morphometric analysis of the lumbar intervertebral foramen in patients with degenerative lumbar scoliosis by multidetector-row computed tomography. Eur Spine J 2012;21(12):2594–2602. DOI: 10.1007/s00586-012-2408-7.
5. Amonoo-Kuofi HS, El-Badawi MG, Fatani JA. Ligaments associated with lumbar intervertebral foramina. J Anat 1988;159:1–10. DOI: 10.1097/BRS.0000000000000371.
6. Senoo I, Espinoza Orías AA, An HS, et al. In vivo 3-dimensional morphometric analysis of the lumbar foramen in healthy subjects. Spine (Phila Pa 1976) 2014;39(16):929–935. DOI: 10.7860/IJARS/2018/34903:2379.
7. Choubey AK, Sahni H, Bhatia M, et al. MR morphometry of lumbar spine. Int J Anat Radiol Surg 2018;7(2):RO14–RO19. DOI: 10.7860/IJARS/2018/34903:2379.
8. Magnuson PB. Differential diagnosis of causes of pain in the lower back accompanied by sciatic pain. J Nerv Ment Dis 1946;103(3):305. DOI: 10.1097/00000658-194406000-00008.
9. Larmon WA. An anatomic study of the lumbosacral region in relation to low back pain and sciatica. Ann Surg 1994;119(6):892–896. DOI: 10.1097/00000658-194406000-00009.
10. Bulyshchenko GG, Gaivoronskii AI, Gaivoronskii IV. Morphoscopic and morphometric characteristics of intervertebral foramina in the lumbar segment of the spine. Neurosci Behav Physiol 2018;48(5):582–587. DOI: 10.1007/s11055-018-0620-6.
11. Yan S, Zhang Y, Wang K, et al. Three-dimensional morphological characteristics of lower lumbar intervertebral foramen with age. Biomed Res Int 2018;2018:8157061. DOI: 10.1155/2018/8157061.
12. Kırdar L, Training K. Measurement of lumbar intervertebral disc heights by computed tomography: Morphometric study. J Turk Spinal Surg 2015;26(4):289–292. DOI: 10.4328/JCAM.3212.
13. Agichani SR, Joshi SD, Joshi SS. Morphometric study of lumbar intervertebral discs in a tertiary care center in central India. J Evid Based Med Healthc 2021;8(31):2895–2899. DOI: 10.18410/jebmh/2021/529.
14. Çetin T, Kahraman S, Kızılgöz V, et al. The comparison between herniated and non-herniated disc levels regarding intervertebral disc space height and disc degeneration: A magnetic resonance study. Diagnostics 2023;13:3190. DOI: 10.3390/diagnostics13183190.
15. Gkasdaris G, Hourmouzi D, Chaniotakis C, et al. CT assessment of the in vivo osseous lumbar intervertebral foramen: A radiologic study with clinical applications. Maedica (Bucur) 2018;13(4):294. DOI: 10.26574/maedica.2018.13.4.294.
16. Al-Hadidi MT, Abu-Ghaida JH, Badran DH, et al. Magnetic resonance imaging of normal lumbar intervertebral foraminal height. Saudi Med J 2003;24(7):736–741. PMID: 12883604.
17. Twomey L, Taylor J. Age changes in the lumbar spinal and intervertebral canals. Paraplegia 1988;26(4):238–249. DOI: 10.1038/sc.1988.37.
18. Bonnheim NB, Lazar AA, Kumar A, et al. ISSLS prize in bioengineering science 2023: Age- and sex-related differences in lumbar intervertebral disc degeneration between patients with chronic low back pain and asymptomatic controls. Eur Spine J 2023;32(5):1517–1524. DOI: 10.1007/s00586-023-07542-6.
19. Lee S, Lee JW, Yeom JS, et al. A practical MRI grading system for lumbar foraminal stenosis. Am J Roentgenol 2010;194(4):1095–1098. DOI: 10.2214/AJR.09.3374.

ORIGINAL RESEARCH

Age-wise Comparative Study of Corneal Morphometry and Histology in Human Cadavers and Its Implications for Surgical Planning and Treatment

Shashwat Singh[1], Nityanand Srivastava[2], Jyoti Sharma[3], Monika Srivastava[4], Vishal R Jasuja[5]

Received on: 09 December 2025; *Accepted on:* 01 January 2026; *Published on:* 20 January 2026

Abstract

Background: The cornea is a transparent, avascular tissue whose morphometry and microstructural characteristics undergo dynamic changes with age. Recognizing these normal age-related variations is crucial not only for optimizing ophthalmic interventions such as refractive surgery, keratoplasty, and cataract procedures, but also for establishing the cornea as a potential biomarker in systemic and neurological disorders.

Materials and methods: A cross-sectional cadaveric study was conducted on 30 corneal specimens (10 fetus, 10 adults, and 10 elderly). Gross morphometry included horizontal and vertical corneal diameters (VCDs), central and peripheral thickness, and circumference, measured with digital calipers. Histological analysis was performed with hematoxylin and eosin (H&E) staining to assess the changes.

Results: The study demonstrated a progressive thinning of the central cornea with age, while the peripheral quadrants, particularly the nasal and inferior regions, showed relative thickening. The temporal quadrant revealed pronounced thinning in the elderly. Hematoxylin and eosin stain indicates structural changes from fetal to elderly stages, with progressive maturation, and degeneration across all layers. Our findings mirror with other authors studies, underscoring the reliability of postmortem morphometry in age-related corneal changes.

Conclusion: Horizontal corneal diameter (HCD) guides intraocular lens (IOL) sizing and contact lens fitting; vertical diameter helps detect corneal anomalies; central thickness is key for refractive surgery and glaucoma assessment; superior and inferior thicknesses aid in biomechanical and keratoconus evaluation; nasal and temporal thicknesses assist in graft stability and peripheral assessment; corneal circumference supports surgical planning and prosthetic design. This study establishes the clinical and surgical relevance of corneal parameters for precise ophthalmic care.

Keywords: Age-related changes, Cadaveric study, Cornea, Histology, Morphometry.

Journal of Anatomical Sciences (2025): 10.5005/jas-11049-0011

Introduction

The cornea is a transparent, avascular, and highly specialized tissue that plays a pivotal role in maintaining both the refractive power and optical clarity of the eye. As the principal refractive surface, its morphometric and histological integrity is indispensable for normal vision. Structurally, the cornea consists of five well-defined layers: Epithelium, Bowman's layer, stroma, Descemet's membrane, and endothelium, each contributing uniquely to transparency, hydration control, and biomechanical strength.[1,2]

Age-related variations in corneal morphology and microstructure are well recognized but remain incompletely characterized. Subtle yet progressive epithelial thinning, stromal remodeling, and endothelial cell loss gradually impair the transparency and refractive stability. The clinical consequences of these changes extend well beyond anatomical interest, influencing surgical outcomes and visual prognosis.[3,4]

In ophthalmology, they form the basis of critical disorders such as keratoconus, presbyopia, glaucoma, and corneal dystrophies, where even minute deviations in the cornea can translate into profound visual disability.[5,6] Emerging evidence positions the cornea as a "window to the nervous system," where quantifiable alterations in microstructural integrity mirror the progression of systemic neurodegenerative disorders such as diabetes mellitus, multiple sclerosis, and Parkinson's disease.[7] The cornea is no longer just an optical window; it is a neurological mirror, reflecting silent disease long before symptoms surface.[8]

[1–5]Department of Anatomy, Uttar Pradesh University of Medical Sciences, Saifai, Uttar Pradesh, India

Corresponding Author: Monika Srivastava, Department of Anatomy, Uttar Pradesh University of Medical Sciences, Saifai, Uttar Pradesh, India, Phone: +91 9554149490, e-mail: monikasrivastava1981@gmail.com

How to cite this article: Singh S, Srivastava N, Sharma J, *et al*. Age-wise Comparative Study of Corneal Morphometry and Histology in Human Cadavers and Its Implications for Surgical Planning and Treatment. J Anat Sciences 2025;33(2):38–45.

Source of support: Nil

Conflict of interest: None

Corneal morphometry is traditionally assessed using non-invasive tools like ultrasound pachymetry, optical pachymetry, and AS-OCT, which provide surface measurements thickness and curvature but are restricted to surface evaluation with no histological insight.[9]

Cadaveric analysis, in contrast, offers a rare opportunity to go beyond imaging, allowing direct morphometric measurements to be correlated with histological details. This dual approach not only strengthens the validity of *in vivo* observations but also uncovers age-related microstructural alterations that are otherwise not approachable, thereby expanding our understanding of the cornea on a deeper level.[10]

The urgency of such research is underscored by the growing burden of corneal blindness and the rising prevalence of age-associated ocular and neurodegenerative disorders worldwide. The demand for precise surgical interventions, reliable prognostic markers, and individualized treatment strategies is greater than ever.

Globally, nearly 1,00,000 corneal transplants are performed each year, yet over 12 million patients remain untreated; in India, only 25,000–30,000 surgeries are done annually against a need of nearly 1,00,000. Despite this burden, cadaveric studies on age-related corneal morphometry and histology remain scarce, especially in the Indian population, where genetic and environmental factors may influence ocular anatomy.

This study was therefore undertaken to evaluate corneal changes across age-groups and correlate them with clinical relevance, refining ophthalmic surgical planning, enhancing refractive and cataract outcomes, and supporting early detection of neurologic disorders.

Novelty

This study is the first of its kind to integrate histological and morphometric analyses of the human cornea. Combining microscopic tissue evaluation with precise structural measurements provides a comprehensive understanding of corneal architecture.

Previous studies have explored these aspects separately, but none have correlated them within the same dataset in detail.

The findings establish a modern baseline for corneal parameters for the current population.

This integrated approach offers new insights into corneal anatomy, variability, and adaptation.

Such data are vital for enhancing contact lens fitting, refractive surgery planning, and biomechanical modeling.

Overall, this research introduces a novel framework that bridges laboratory analysis with clinical application, setting the stage for more personalized ocular care.

Materials and Methods

Study Design and Ethical Approval

This cross-sectional cadaveric study was conducted in the Department of Anatomy, Uttar Pradesh University of Medical Sciences, Saifai, Uttar Pradesh, during the academic year 2024–2025. Ethical clearance was obtained from the Institutional Ethics Committee (Ethical Number—239/RC/UPUMS/2024 – 2025), and all procedures were performed in accordance with the ethical standards of the Declaration of Helsinki (2013 revision).[11]

Specimen Collection and Grouping

A total of 30 corneal specimens were obtained, comprising three distinct groups with 10 specimens in each group:

1. Fetal group: 25–30 weeks.
2. Adult group: 18–60 years.
3. Elderly: >60 years.

Age Confirmation

- Fetal gestational age was determined using crown-rump length, biparietal diameter (BPD), head circumference (HC), abdominal circumference (AC), and validated with standard fetal growth charts.
- The adult and elderly cadavers age was confirmed by dental examination, other available identifiers such as postmortem documentation, institutional archives, and official identity records.

Inclusion Criteria

- Gross features appeared normal.
- Cadavers that were embalmed within 24 hours.
- Cadavers with an embalming period of under 5 years.

Exclusion Criteria

- Documented history of neurological disorders.
- Presence of ocular pathology, including congenital or acquired abnormalities.
- History of ocular trauma or intraocular surgery.
- Known cases of diabetes mellitus or systemic hypertension.

Sample Size Calculation Formula (for One-way ANOVA)

- Purposive (nonprobability) sampling.

Parameters Used in Software-based Calculation

- Effect size (f): 0.4 (moderate, as per Cohen's criteria)
- α (type I error): 0.05
- Power ($1 - \beta$): 0.80
- Number of groups (k): 3

Using these parameters in G*Power gives total sample size = 27 (i.e., 9 per group). Rounded up to 30 (10 per group) to enhance statistical reliability.

Statistical Analysis

The collected data were analyzed using IBM SPSS Statistics version 31. Mean values and standard deviations were calculated for corneal parameters, including central corneal thickness (CCT), corneal diameter, epithelial thickness, stromal thickness, and endothelial cell count across different age-groups (infant, adult, and elderly). The results were compared descriptively to identify age-related trends in corneal morphometry and histology. Differences observed between the groups were presented using approximate p-values where applicable. The results were also compared with previous studies using alternative methodologies, and areas of concordance were noted.

Methodology

Methodology Steps

- Gross dissection.
- Histology stain via hematoxylin and eosin (H&E) stain.

Gross Morphometric Analysis

Dissection of the cornea was carried out according to the standard protocol outlined in Cunningham's manual of Practical Anatomy.[12] The eyeballs were carefully removed from the orbital cavities and gently dissected away the surrounding fat and extraocular muscles to obtain a clean globe, except for the lateral rectus stump to identify the side of the eyeball.

Anatomical landmarks, including the cornea scleral junction (limbus) and equator of the eyeball, were identified for orientation. Gross morphometric measurements were subsequently performed.

A circumferential incision was then made at the equator, separating the globe into anterior and posterior segments. The cornea was carefully delineated from the sclera at the limbus,

Fig. 1: Horizontal diameter of cornea

Fig. 3: Central corneal thickness measurement

Fig. 2: Vertical diameter of cornea

Fig. 4: Peripheral corneal thickness measurement

ensuring that the natural curvature and transparency were preserved for further gross and histological examination.

The measurements were performed by three operators. Each operator made five measurements for each dimension. The time taken by each operator to complete the measurements was approximately 10 minutes. To reduce operator bias, one operator adjusted the calipers for measurements, and the values were read and recorded by a different operator.

Gross Measurement Parameters

- Horizontal corneal diameter (HCD): Measured from limbus-to-limbus along the horizontal axis (3–9 o'clock) (Fig. 1).
- Vertical corneal diameter (VCD): Measured from limbus-to-limbus along the vertical axis (12–6 o'clock) (Fig. 2).
- CCT: Measured at the center of the cornea using a Vernier caliper (anterior to posterior surface) (Fig. 3).
- Superior corneal thickness (SCT): Thickness of the cornea measured in the superior quadrant, near the limbus (12 o'clock position) (Fig. 4).
- Inferior corneal thickness (ICT): Thickness of the cornea measured in the inferior quadrant, near the limbus (6 o'clock position) (Fig. 4).
- Nasal corneal thickness (NCT): Thickness of the cornea measured in the nasal quadrant, toward the nose (3 o'clock in the right eye, 9 o'clock in the left eye) (Fig. 4).
- Temporal corneal thickness (TCT): Thickness of the cornea measured in the temporal quadrant, toward the temple (opposite the nasal side) (Fig. 4).
- Corneal circumference: The total distance around the cornea, usually estimated from the HCD using the formula $C = \pi \times$ HCD. [HCD is generally preferred because the cornea is slightly oval, and HCD provides a more accurate and clinically relevant estimate in corneal surgery planning, intraocular lens (IOL) sizing, and contact lens fitting.]

Histological Examination (H&E Stain)

After gross measurements, corneal specimens were fixed in 10% formalin, processed through routine paraffin embedding, and sectioned at 5–7 µm thickness. Sections were stained with H&E and further analyzed.[13]

- Epithelium: Cell layers, cell morphology.
- Bowman's layer: Presence, organization, integrity.
- Stroma: Collagen organization, keratocyte density.

- Descemet's membrane: Maturity, posterior deposits.
- Endothelium: Cell density, shape (pleomorphism), size variation (polymegathism).

Results

Gross Result

The cornea undergoes a remarkable developmental transformation from the fetal period to adulthood, followed by subtle age-related changes in the elderly.

Corneal parameters, including horizontal and vertical diameters, central and peripheral thicknesses, and overall circumference which serve as the gold standard for comprehensive corneal assessment in modern ophthalmology.

Horizontal corneal diameter (HCD) increases from 10.2 ± 0.4 mm in fetuses to 11.8 ± 0.5 mm in adults, with a minor decline to 11.6 ± 0.4 mm in the elderly. The *p*-value was found to be significant, as *p*-value < 0.001, stating a true developmental increase with mild age-related reduction. This parameter is important for IOL selection, keratoplasty, and refractive surgery such as LASIK or SMILE, as it determines the horizontal corneal span and helps optimize grafts or lens coverage (Table 1 and Fig. 1).

Vertical corneal diameter (VCD) rises from 9.8 ± 0.3 mm in fetuses to 11.5 ± 0.5 mm in adults, decreasing slightly to 11.4 ± 0.4 mm in the elderly. The *p*-value was found to be significant, as *p*-value < 0.001, stating substantial postnatal growth with mild age-related decrease. This parameter is important for contact lens fitting, detecting vertical asymmetries, and monitoring ocular growth and congenital anomalies along the vertical axis (Table 1 and Fig. 2).

Central corneal thickness decreases from 0.64 ± 0.02 mm in fetuses to 0.55 ± 0.02 mm in adults, with a slight reduction to 0.54 ± 0.02 mm in the elderly. The *p*-value was found to be significant, as *p*-value < 0.001, stating normal developmental with age-related thinning. This parameter is important for accurate intraocular pressure measurement in glaucoma, planning refractive surgeries like LASIK, detecting corneal disorders such as keratoconus or edema, and guiding contact lens fitting (Table 1 and Fig. 3).

Superior corneal thickness increases from 0.56 ± 0.01 mm in fetuses to 0.69 ± 0.05 mm in adults, decreasing slightly to 0.59 ± 0.01 mm in the elderly. The *p*-value was found to be significant, as *p*-value < 0.01, stating postnatal thickening with mild age-related thinning. This parameter is important for detecting regional thinning, planning sectoral corneal procedures, and optimizing contact lens fit (Table 1 and Fig. 4).

Inferior corneal thickness rises from 0.56 ± 0.02 mm in fetuses to 0.74 ± 0.06 mm in adults, slightly reducing to 0.71 ± 0.025 mm in the elderly. The *p*-value was found to be significant, as *p*-value < 0.01, stating normal postnatal growth with mild age-related thinning. This parameter is useful for inferior corneal surgical planning, monitoring regional corneal changes, and identifying early keratoconus or oedema (Table 1 and Fig. 4).

Nasal corneal thickness grows from 0.55 ± 0.01 mm in fetuses to 0.74 ± 0.05 mm in adults, with a minor decline to 0.71 ± 0.022 mm in the elderly. The *p*-value was found to be significant, as *p*-value < 0.01, stating postnatal growth with age-related thinning. This parameter is relevant for nasal corneal interventions, regional disease detection, and contact lens fitting (Table 1 and Fig. 4).

Temporal corneal thickness (TCT) increases from 0.55 ± 0.017 mm in fetuses to 0.74 ± 0.055 mm in adults, slightly decreasing to 0.72 ± 0.020 mm in the elderly. The *p*-value was found to be significant, as *p*-value < 0.01, stating postnatal growth with mild age-related thinning. This parameter is important for temporal corneal assessment, surgical planning, and preventing lens edge-related complications (Table 1 and Figs 4 to 6).

Table 1: Mean corneal measurements across different age-groups

Parameter	*Fetal (25–30 weeks)*	*Adult (18–60 years)*	*Elderly (>60 years)*	*p-value*
HCD (mm)	10.2 ± 0.4	11.8 ± 0.5	11.6 ± 0.4	<0.001
VCD (mm)	9.8 ± 0.3	11.5 ± 0.5	11.4 ± 0.4	<0.001
CCT (mm)	0.64 ± 0.02	0.55 ± 0.02	0.54 ± 0.02	<0.001
SCT (mm)	0.56 ± 0.01	0.69 ± 0.05	0.59 ± 0.01	<0.01
ICT (mm)	0.56 ± 0.02	0.74 ± 0.06	0.71± 0.025	<0.01
NCT (mm)	0.55 ± 0.01	0.74 ± 0.05	0.71 ± 0.022	<0.01
TCT (mm)	0.55 ± 0.017	0.74 ± 0.055	0.72 ± 0.020	<0.01
Corneal circumference ($C = \pi \times HCD$)	31.95 ± 1.26	37.05 ± 1.57	36.45 ± 1.26	<0.001

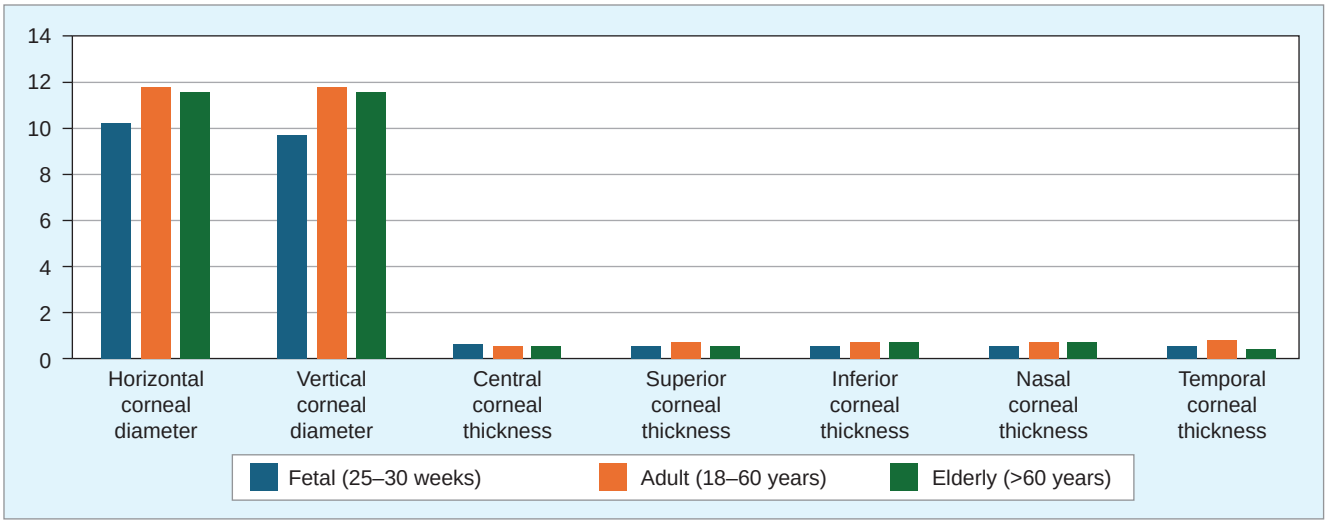

Fig. 5: Bar representation of corneal morphometric parameters across three age-groups

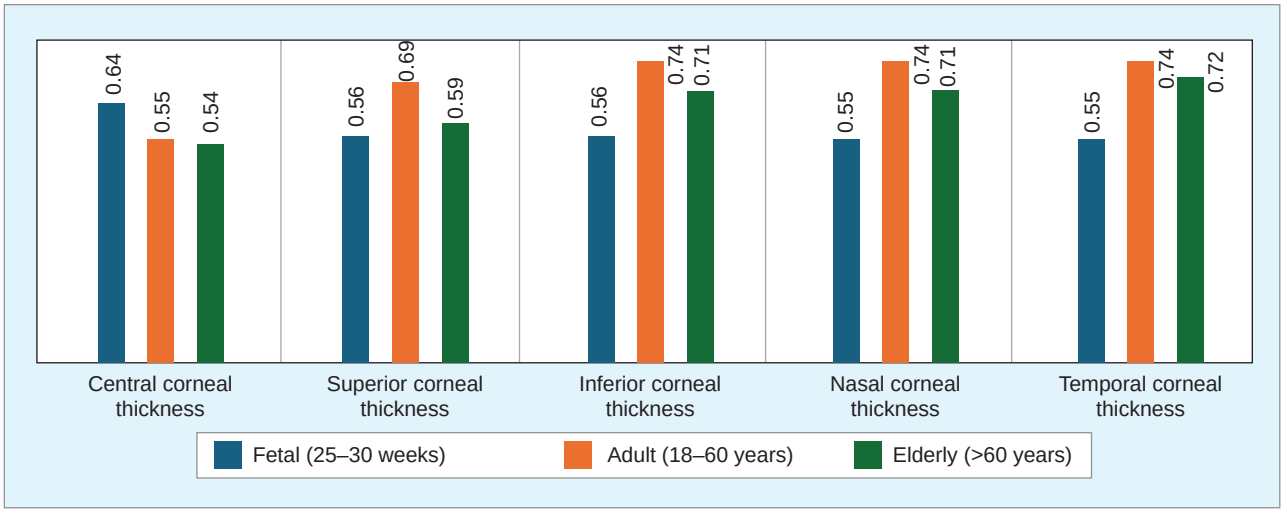

Fig. 6: Bar representation of different corneal thicknesses across three age-groups

Table 2: Left and right cornea mean measurements across different age-groups

Parameter	*Fetal (25–30 weeks)*	*Adult (18–60 years)*	*Elderly (>60 years)*
HCD (mm)	R: 10.20 ± 0.4	R: 11.79 ± 0.32	R: 11.61 ± 0.31
	L: 10.20 ± 0.4	L: 11.78 ± 0.31	L: 11.59 ± 0.32
VCD (mm)	R: 9.82 ± 0.3	R: 11.50 ± 0.34	R: 11.41 ± 0.32
	L: 9.81 ± 0.3	L: 11.50 ± 0.33	L: 11.39 ± 0.33
CCT (mm)	R: 0.64 ± 0.02	R: 0.55 ± 0.02	R: 0.54 ± 0.02
	L: 0.64 ± 0.02	L: 0.54 ± 0.02	L: 0.54 ± 0.02
SCT (mm)	R: 0.56 ± 0.01	R: 0.69 ± 0.055	R: 0.59 ± 0.016
	L: 0.55 ± 0.01	L: 0.69 ± 0.055	L: 0.58 ± 0.016
ICT (mm)	R: 0.56 ± 0.02	R: 0.74 ± 0.06	R: 0.71 ± 0.025
	L: 0.56 ± 0.02	L: 0.74 ± 0.06	L: 0.71 ± 0.025
NCT (mm)	R: 0.55 ± 0.01	R: 0.74 ± 0.05	R: 0.71 ± 0.022
	L: 0.54 ± 0.01	L: 0.73 ± 0.05	L: 0.71 ± 0.022
TCT (mm)	R: 0.55 ± 0.017	R: 0.74 ± 0.055	R: 0.72 ± 0.020
	L: 0.55 ± 0.017	L: 0.74 ± 0.055	L: 0.71 ± 0.020

Table 3: Sequence of corneal thickness across three age-groups

Age-group	*Sequence of thickness (Highest → Lowest)*
Fetal	Central > Superior ≈ Inferior > Nasal ≈ Temporal
Adult	Inferior ≈ Nasal ≈ Temporal > Superior > Central
Elderly	Nasal > Inferior > Superior > Central > Temporal

Table 4: Histological comparison of corneal layers across age-groups

Corneal layer	*Fetal (25–30 weeks) (Fig. 7)*	*Adult (18–60 years) (Fig. 8)*	*Elderly (>60 years) (Fig. 9)*
Epithelium	• Thin, predominantly basal cells • Stratification begins	• Fully stratified • All layers developed • Well-differentiated	• Slight thinning; decreased regenerative capacity
Bowman's layer	• Rudimentary or absent	• Fully formed • Acellular	• Fragmentation or thickening may occur
Stroma	• Less organized collagen • High cellularity • Keratocytes abundant	• Well-organized lamellae • Moderate keratocyte density	• Collagen lamellae irregular • Keratocyte number declines • Mild stromal edema possible
Descemet's membrane	• Very thin • Immature	• Thickened and strong basement membrane for endothelium	• Progressive thickening
Endothelium	• Monolayer present • Cells are large and irregular	• Regular hexagonal monolayer • Maintains transparency	• Reduced cell density • Pleomorphism and polymegathism

Corneal circumference ($C = \pi \times HCD$) increases from 31.95 ± 1.26 mm in fetuses to 37.05 ± 1.57 mm in adults, with a slight decrease to 36.45 ± 1.26 mm in the elderly. The *p*-value was found to be significant, as *p*-value < 0.001, stating overall corneal growth with mild age-related reduction. This parameter is important for planning corneal and refractive surgeries, customizing contact lenses, and assessing overall corneal size for diagnostic and anthropometric studies (Table 1).

Corneal morphometry showed progressive growth from fetal to adult life, with slight thinning in the elderly. The right eye consistently exhibited slightly larger diameters and thicknesses than the left, with differences around 0.01–0.02 mm across HCD, VCD, CCT, and regional thicknesses. These findings highlight normal developmental trends and subtle anatomical asymmetry, providing a precise reference for ophthalmic assessment and surgical planning (Tables 2 and 3).

These parameters not only enable tailored keratoplasty, refractive surgery, and contact lens customization, but also allow early detection of subtle corneal anomalies and accurate glaucoma risk assessment. By integrating developmental, regional, and global corneal metrics, this study transforms corneal evaluation from routine measurement into a predictive, patient-specific tool, setting a new standard for ocular care (Tables 4 and 5).

Table 5: Discussion overview

Study	*Year*	*Population*	*Subjects*	*Method*	*Mean diameters (mm)*	*Measurement site*	*Gross observations*	*Histological observations*
Rüfer et al.[14]	2007	Germany	370 Patients	Orbscan II topography	11.71 ± 0.42	HCD	HCD > VCD	NA
Hashemi et al.[15]	2012	Iran	4,787 patients	Biometry	11.80 ± 0.23	Mean WTW corneal diameter	HCD > VCD WTW changes with age	NA
Merhar and Naicker[10]	2020	Hyderabad	Postmortem eyeballs	Vernier caliper	11.94 ± 0.16 11.45 ± 0.05	Horizontal and vertical globe	HCD > VCD	NA
Taurone et al.[16]	2020	Italy	20 postmortem	Light microscopy	NA	Whole cornea	NA	Adult: Hexagonal cells present. normal stromal thickness Old age: Cell loss and swelling, thinned and reduced stroma
Singh et al. (present study)	2025	Fetal, adult, elderly	30 eyeballs	Vernier caliper + light microscope	HCD: 11.8 ± 0.5 VCD: 11.5 ± 0.5	Horizontal, vertical, center, peripheral	HCD > VCD Decline in elderly peripheral thickness variations present	Fetus: Stratification starts Adult: Hexagonal cells, strong basement layer Old age: Cell loss, fragmentation and thickening

Histology Result

Refer to Figures 7 to 9.

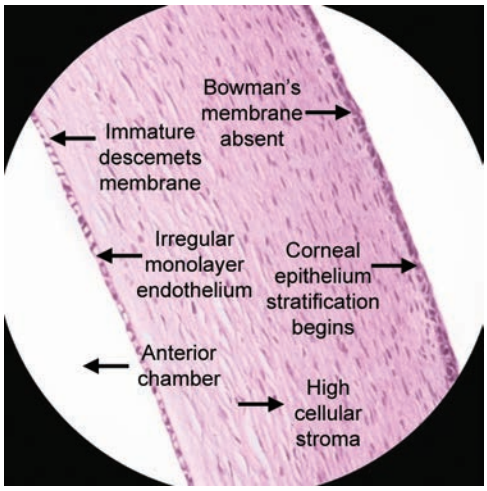

Fig. 7: (H&E stain, ×40) fetal human cornea

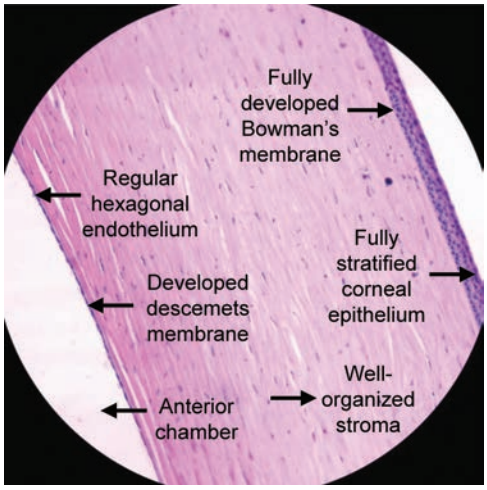

Fig. 8: (H&E stain, ×40) histology of the normal adult cornea

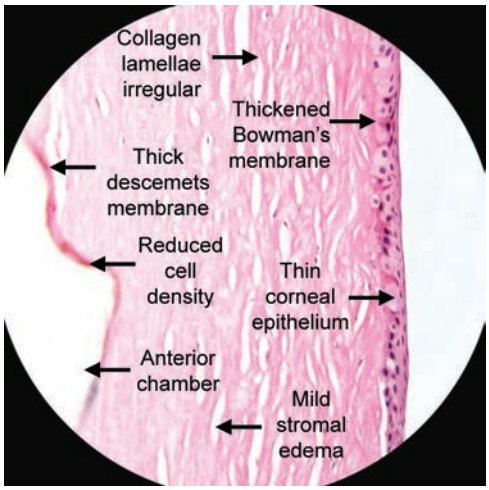

Fig. 9: (H&E stain, ×40) normal old age cornea

Discussion

In our study, the HCD increased from 10.2 ± 0.4 mm in fetuses to 11.8 ± 0.5 mm in adults, with a slight decline to 11.6 ± 0.4 mm in the elderly. This developmental enlargement, followed by a mild reduction, is similar to the findings of Rüfer et al.,[14] who reported an average corneal diameter of 11.71 ± 0.42 mm in adults, and Gharaee et al.,[17] who observed similar values in an Iranian population. The minor decline in elderly groups is consistent with age-related ocular surface changes described by Hashemi et al.[15]

The VCD in our study showed a parallel growth pattern, rising from 9.8 ± 0.3 mm in fetuses to 11.5 ± 0.5 mm in adults, with a slight reduction to 11.4 ± 0.4 mm in the elderly. Augusteyn et al.[18] demonstrated that horizontal expansion of the cornea exceeds vertical expansion, a finding corroborated by our results, where VCD values were consistently lower than HCD values across all age-groups.

Central corneal thickness in our study showed a marked reduction from 0.64 ± 0.02 mm in fetuses to 0.55 ± 0.02 mm in

adults, with a further decline to 0.54 ± 0.02 mm in the elderly. These findings echo reports by Rushood et al.,[19] who found neonatal CCT to be thicker compared to adults, and by Ecsedy et al.,[20] who showed progressive thinning during postnatal development. Hekimoglu et al.[21] also reported higher CCT in preterm infants (~630 µm), which converged towards adult averages, supporting our observations.

The SCT in our series increased from 0.56 ± 0.01 mm in fetuses to 0.69 ± 0.05 mm in adults, with a decline to 0.59 ± 0.01 mm in the elderly. Regional variations in corneal thickness have been well established, and our results are in line with studies by Doughty and Zaman,[22] who highlighted that the superior cornea tends to be thicker than the central portion, with age-related thinning occurring in later decades.

Similarly, the ICT increased from 0.56 ± 0.02 mm in fetuses to 0.74 ± 0.06 mm in adults, decreasing slightly to 0.71 ± 0.025 mm in the elderly. This pattern of relative inferior thickening is supported by the work of Randleman et al.,[23] who showed that ICT measurements are critical for detecting early keratoconus. The small age-related thinning seen in our material is consistent with corneal biomechanical changes described by Kamiya et al.[24]

The NCT showed an increase from 0.55 ± 0.01 mm in fetuses to 0.74 ± 0.05 mm in adults, with a slight reduction to 0.71 ± 0.022 mm in the elderly. Regional asymmetries have also been documented by Huang et al.,[25] who demonstrated thicker nasal corneas compared to temporal quadrants, which is in accordance with our findings.

Finally, the TCT increased from 0.55 ± 0.017 mm in fetuses to 0.74 ± 0.055 mm in adults, with a slight decrease to 0.72 ± 0.020 mm in the elderly. Our values are consistent with the pattern described by Doughty and Zaman,[22] who noted that the temporal region is thicker than the central cornea but generally thinner than the nasal quadrant. When corneal circumference was calculated from HCD values, we observed an increase from 31.95 ± 1.26 mm in fetuses to 37.05 ± 1.57 mm in adults, followed by a minor decline in the elderly. This reflects overall growth of the cornea and parallels the biometric observations of Augusteyn et al.,[18] who described corneal growth as a gradual process stabilizing after adolescence.

Our histological study shows close similarity to the findings of Taurone et al.[16] In both studies, elderly corneas demonstrated epithelial thinning with reduced regenerative capacity, stromal remodeling with a decline in keratocyte number, and progressive thickening of Descemet's membrane often associated with posterior collagenous deposits. Likewise, both sets of observations confirm a marked reduction in endothelial cell density, accompanied by pleomorphism and polymegathism, ultimately compromising corneal transparency.

Conclusion

In Academics

Age-related corneal changes highlight the need for age-stratified normative datasets to strengthen research and future innovations.

In Ophthalmology

Refine diagnosis, improve refractive accuracy, and guide safer surgical planning.

In Surgical

Enables tailored techniques, better IOL power prediction, and ultimately improving surgical safety and outcomes.

Limitation

- Potential artifactual shrinkage from formalin fixation was excluded as our study finding correlates with other radiological studies, ensuring highly accurate data.
- Although the sample size was modest, the study provides the same valuable measurements as a radiological study, which is applicable to clinical practice.

Orcid

Shashwat Singh https://orcid.org/0009-0002-3833-4084

References

1. Sridhar MS. Anatomy of cornea and ocular surface. Indian J Ophthalmol 2018;66(2):190–194. DOI: 10.4103/ijo.IJO_646_17.
2. Eghrari AO, Riazuddin SA, Gottsch JD. Overview of the cornea: Structure, function, and development. Prog Mol Biol Transl Sci 2015;134:7–23. DOI: 10.1016/bs.pmbts.2015.04.001.
3. Galgauskas S, Norvydaitė D, Krasauskaitė D, et al. Age-related changes in corneal thickness and endothelial characteristics. Clin Interv Aging 2013;8:1445–1450. DOI: 10.2147/CIA.S51693.
4. Islam QU, Saeed MK, Mehboob MA. Age related changes in corneal morphological characteristics of healthy Pakistani eyes. Saudi J Ophthalmol 2017;31(2):86–90. DOI: 10.1016/j.sjopt.2017.02.009.
5. Asimellis G, Kaufman EJ. Keratoconus. In: StatPearls. Treasure Island, FL: StatPearls Publishing; 2025. [Updated 2024 Apr 12].
6. Gordon-Shaag A, Millodot M, Shneor E, et al. The genetic and environmental factors for keratoconus. Biomed Res Int 2015;2015:795738. DOI: 10.1155/2015/795738.
7. Petropoulos IN, John K, Al-Shibani F, et al. Corneal immune cells as a biomarker of inflammation in multiple sclerosis: A longitudinal study. Ther Adv Neurol Disord 2023;16:17562864231204974. DOI: 10.1177/17562864231204974.
8. Borsook D. Neurological diseases and pain. Brain 2012;135(Pt 2):320–344. DOI: 10.1093/brain/awr271.
9. Kim HY, Budenz DL, Lee PS, et al. Comparison of central corneal thickness using anterior segment optical coherence tomography vs ultrasound pachymetry. Am J Ophthalmol 2008;145(2):228–232. DOI: 10.1016/j.ajo.2007.09.030.
10. Shapiro L, editor. Microscopy techniques for biomedical education and healthcare practice: Principles in light, fluorescence, super-resolution and digital microscopy, and medical imaging [internet]. Cham: Springer Cham; 2023. Merhar V, Naicker T. pp. 25–40. DOI: 10.1007/978-3-031-36850-9_2.
11. World Medical Association. World Medical Association Declaration of Helsinki: Ethical principles for medical research involving human subjects. JAMA 2013;310(20):2191–2194. DOI: 10.1001/jama.2013.281053.
12. Koshi R. Cunningham's Manual of Practical Anatomy, Volume 3: Head, Neck and Brain. 16th ed. Oxford: Oxford University Press; 2018.
13. Singh D. Principles and Techniques in Histology, Microscopy and Photomicrography. 2nd ed. Kindle Edition. New Delhi: Jaypee Brothers Medical Publishers; 2020.
14. Rüfer F, Schröder A, Erb C. White-to-white corneal diameter: Normal values in healthy humans obtained with the Orbscan II topography system. Cornea 2005;24(3):259–261. DOI: 10.1097/01.ico.0000148312.01805.53.
15. Hashemi H, KhabazKhoob M, Yazdani K, et al. White-to-white corneal diameter in the Tehran Eye Study. Cornea 2010;29(1):9–12. DOI: 10.1097/ICO.0b013e3181a9d0a9.
16. Taurone S, Miglietta S, Spoletini M, et al. Age related changes seen in human cornea in formalin fixed sections and on biomicroscopy in living subjects: A comparison. Clin Anat 2020;33(2):245–256. DOI: 10.1002/ca.23488.

17. Gharaee H, Abrishami M, Shafiee M, et al. White-to-white corneal diameter: Normal values in healthy Iranian population obtained with the Orbscan II. Int J Ophthalmol 2014;7(2):309–312. DOI: 10.3980/j.issn.2222-3959.2014.02.20.
18. Augusteyn RC, Nankivil D, Mohamed A, et al. Human ocular biometry. Exp Eye Res 2012;102:70–75. DOI: 10.1016/j.exer.2012.06.009.
19. Rushood AA, Zahrani MH, Khamis A, et al. Central corneal thickness in full-term Saudi newborns. Acta Ophthalmol 2012;90(5):e355–e358. DOI: 10.1111/j.1755-3768.2012.02412.x.
20. Ecsedy M, Kovacs I, Mihaltz K, et al. Scheimpflug imaging for long-term evaluation of optical components in Hungarian children with a history of preterm birth. J Pediatr Ophthalmol Strabismus 2014;51(4):235–241. DOI: 10.3928/01913913-20140521-04.
21. Hekimoglu E, Erol MK, Toslak D, et al. Comparison of measurement of central corneal thickness with spectral domain optical coherence tomography and standard ultrasonic pachymeter in premature infants. J Ophthalmol 2015;2015:129269. DOI: 10.1155/2015/129269.
22. Doughty MJ, Zaman ML. Human corneal thickness and its impact on intraocular pressure measures: A review and meta-analysis approach. Surv Ophthalmol 2000;44(5):367–408. DOI: 10.1016/s0039-6257(00)00110-7.
23. Randleman JB, Woodward M, Lynn MJ, et al. Risk assessment for ectasia after corneal refractive surgery. Ophthalmology 2008;115(1):37–50. DOI: 10.1016/j.ophtha.2007.03.073.
24. Kamiya K, Shimizu K, Ohmoto F. Effect of aging on corneal biomechanical parameters using the ocular response analyzer. J Refract Surg 2009;25(10):888–893. DOI: 10.3928/1081597X-20090917-10.
25. Huang D, Tang M, Shekhar R. Mathematical model of corneal surface smoothing after laser refractive surgery. Am J Ophthalmol 2003;135(3):267–278. DOI: 10.1016/s0002-9394(02)01942-6.

ORIGINAL RESEARCH

Revisiting the Sciatic Nerve: A Landmark-based Classification of Division Patterns in Relation to the Ischial Tuberosity

Vandana Tiwari[1], Navita Aggarwal[2], Priti Chaudhary[3]

Received on: 06 December 2025; *Accepted on:* 02 January 2026; *Published on:* 20 January 2026

Abstract

Introduction: Increasing anatomical studies reveal considerable variability in sciatic nerve (SN) division, a factor that complicates orthopedic, neurosurgical, and anesthetic procedures. Conventional classification models often lack precision in localizing the site of bifurcation. This study proposes a novel ischial tuberosity (IT)-based classification of SN division for improved reproducibility and clinical applicability.

Materials and methods: Fifty-eight lower limbs from 29 formalin-fixed adult cadavers were dissected. Only nerves passing below the piriformis (Beaton and Anson type A) were included for subclassification. The distance of bifurcation from IT was measured with a caliper, and the vertical bifurcation level relative to the IT was categorized as: Type A-I (Supra-IT), type A-II (At-IT), type A-III (Infra-IT ≤10 cm), and type A-IV (Infra-IT >10 cm). The frequency of each subtype was recorded, and sex- and side-based differences were analyzed.

Results: Out of 58 limbs, 42 (72.41%) showed extra-pelvic bifurcation (type A). Among these, type A-III bifurcations were most frequent, followed by type A-II, type A-IV, and type A-I. Non-type A variants comprised 27.5%. Although variations were more frequent in males, differences by sex and side were not statistically significant.

Conclusion: The study confirms high variability in SN bifurcation and highlights limitations of conventional models. By employing the IT as a landmark, the proposed classification provides greater consistency and anatomical localization of extrapelvic bifurcation of SN. This system enhances procedural safety and offers a reliable framework for anatomical research and teaching.

Keywords: Anatomical variation, Ischial tuberosity, Nerve bifurcation, Regional anesthesia, Surgical landmarks.

Journal of Anatomical Sciences (2025): 10.5005/jas-11049-0016

Introduction

The sciatic nerve (SN), or nervus ischiadicus, is the largest peripheral nerve in the human body, arising from the anterior rami of L4–S3 segments of the lumbosacral plexus. It exits the pelvis through the greater sciatic foramen (GSN), most commonly inferior to the piriformis muscle (PM), and traverses the gluteal region and posterior thigh before dividing into its terminal branches: The tibial nerve (TN) and common peroneal nerve (CPN).[1,2] These branches supply motor and sensory innervation to the majority of the lower limb. Variations in the course and bifurcation level of the SN have important clinical implications. Aberrant divisions, particularly when occurring proximally, are associated with piriformis syndrome (PS), incomplete SN blocks, and increased risk of procedure-related injury during posterior hip surgery or gluteal interventions.[3] Thus, accurate knowledge of bifurcation patterns is critical for surgeons, anesthesiologists, and radiologists.

The classical Beaton and Anson classification (types A–F) remains widely cited for describing SN-PM relationships (Fig. 1, with type A—where the undivided SN passes inferiorly to the PM—being the most common.[4] Other types describe partial or complete division of the SN that passes above, through, or around the PM. However, this system is limited as it considers only the nerve's relationship to the PM and does not account for the variable level of bifurcation, which can occur anywhere from the pelvis to the popliteal fossa. This variation is particularly relevant in procedures requiring targeted nerve blocks or posterior surgical approaches.[5–7]

Conventional models often lack reproducible anatomical landmarks, limiting comparability across studies. Furthermore, many recently identified patterns of SN division fall outside the classical model, especially with the increased use of high-resolution imaging and meticulous cadaveric dissection.[4,6] To address these gaps, the present study introduces the IT as a reliable bony landmark for classifying SN bifurcation. This landmark-based system offers a morphometrically consistent and clinically meaningful framework, facilitating reproducibility in cadaveric research, precision in diagnostic imaging, and safety in surgical and anesthetic procedures.

[1–3]Department of Anatomy, All India Institute of Medical Sciences, Bathinda, Punjab, India

Corresponding Author: Vandana Tiwari, Department of Anatomy, All India Institute of Medical Sciences, Bathinda, Punjab, India, Phone: +91 9599928294, e-mail: vandana.918in@gmail.com

How to cite this article: Tiwari V, Aggarwal N, Chaudhary P. Revisiting the Sciatic Nerve: A Landmark-based Classification of Division Patterns in Relation to the Ischial Tuberosity. J Anat Sciences 2025;33(2):46–50.

Source of support: Nil

Conflict of interest: None

Materials and Methods

This cadaveric study was conducted over a 6-year period (2019–2024) in the dissection hall of the Department of Anatomy. A total of 58 lower limbs from 29 formalin-fixed cadavers (18 males and 11 females), aged between 45 and 92 years, were examined. All cadavers were obtained through the institute's voluntary body donation program with documented consent specifying their

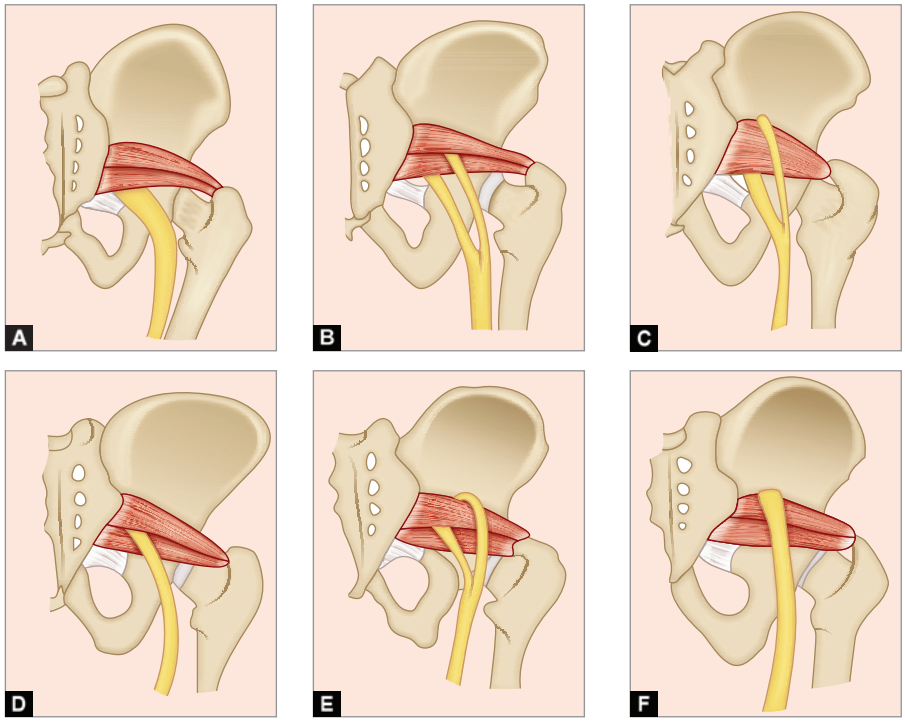

Figs 1A to F: Schematic diagram of six types of the anatomical relationship between the SN and the PM according to Beaton and Anson: (A) Undivided nerve passes below the muscle; (B) Divisions of nerve pass between and below muscle; (C) Divisions of nerve pass above and below the muscle; (D) Undivided nerve passes between the divided heads of the muscle; (E) Divisions of nerve pass between and above the divided muscle; (F) Undivided nerve passes above the muscle

use for educational and research purposes. The specimens were preserved in 10% formalin solution.

Inclusion criteria were intact lower limbs with preserved musculature and bony landmarks of the gluteal and posterior thigh regions. Exclusion criteria included specimens with evidence of trauma, surgical intervention, pathology, or deformity affecting the anatomy of interest.

Dissection was performed with cadavers in the prone position following standard anatomical protocols. After reflecting the skin, superficial fascia, and gluteus maximus, the PM and SN were exposed. The SN was traced distally until its bifurcation into the TN and CPN. For each specimen, the type of SN division was recorded bilaterally using a tabular format in Microsoft Excel. Photographic documentation was obtained using a Nikon Coolpix S3400 camera. To ensure classification accuracy and reduce observer bias, two independent anatomists verified each observation. The IT was used as the primary bony landmark to document the level of bifurcation. Measurements were taken using standard tools—ruler, yarn, and pins—and recorded in millimeters. Each measurement was taken twice, and the average value was used for analysis. Data entry was done in Microsoft Excel. To assess intraobserver reliability, the principal investigator repeated all measurements after 1 month, and the results were compared with initial values.

Proposed Classification System: Ischial Tuberosity (IT)-based Sciatic Nerve Bifurcation Classification (IT-SNBC)

Based on observed variation in extrapelvic SN bifurcation (Beaton and Anson type A), a novel IT-SNBC is proposed to provide a standardized and reproducible framework for anatomical and clinical reference. In this system, type A SN emerging from the pelvis as a single trunk below the piriformis is further subdivided according to its bifurcation level relative to the IT. Bifurcation was classified into four types:

- Type A-I – Supra-IT: Bifurcation proximal to the superior border of the IT.
- Type A-II – At-IT: Bifurcation at the level of the IT.
- Type A-III – Infra-IT (Short thigh): Bifurcation within 0–10 cm distal to the IT.
- Type A-IV – Infra-IT (Long thigh): Bifurcation >10 cm distal to the IT.

This landmark-based system offers a quantitative and location-oriented refinement of type A variants, which are most frequently encountered in clinical practice. By anchoring classification to a reproducible bony landmark, the IT-SNBC enhances anatomical localization, facilitates consistent reporting across studies, and improves applicability in surgical planning, regional anesthesia, radiological interpretation, and anatomical education.

Statistical Analysis

Statistical analysis was performed using IBM SPSS® v29. Frequencies and percentages summarized categorical data, while mean ± SD described numerical variables. Side- and sex-based comparisons were made using Chi-square/Fisher's exact test and unpaired *t*-tests. A p-value < 0.05 was considered statistically significant.

Results

Out of 58 lower limbs, 42 (72.41%) exhibited extra-pelvic bifurcation (type A). Non-type A variants accounted for 27.5% of specimens. While incidence of variation by sex or side was not statistically

Table 1: Prevalence of SN variation types with respect to sex and side

	Males n (%)		*Females n (%)*		*Total n (%)*
Type of SN	*Rt*	*Lt*	*Rt*	*Lt*	
Type A					
Type A-I (Above IT)	0 (0)	3 (16.7)	0 (0)	0 (0)	3 (5.3)
Type A-II (At-IT)	2 (11.1)	4 (22.3)	2 (18.2)	2 (18.2)	10 (17.2)
Type A-III (Infra-IT, 0–10 cm distal)	8 (44.5)	5 (27.7)	4 (36.4)	4 (36.4)	21 (36.2)
Type A-IV (Infra-IT, >10 cm distal)	2 (11.1)	1 (5.6)	3 (27.2)	2 (18.2)	8 (13.8)
Non-type A	6 (33.3)	5 (27.7)	2 (18.2)	3 (27.2)	16 (27.5)
Total	18 (100)	18 (100)	11(100)	11(100)	58 (100)

IT, ischial tuberosity; SN, sciatic nerve

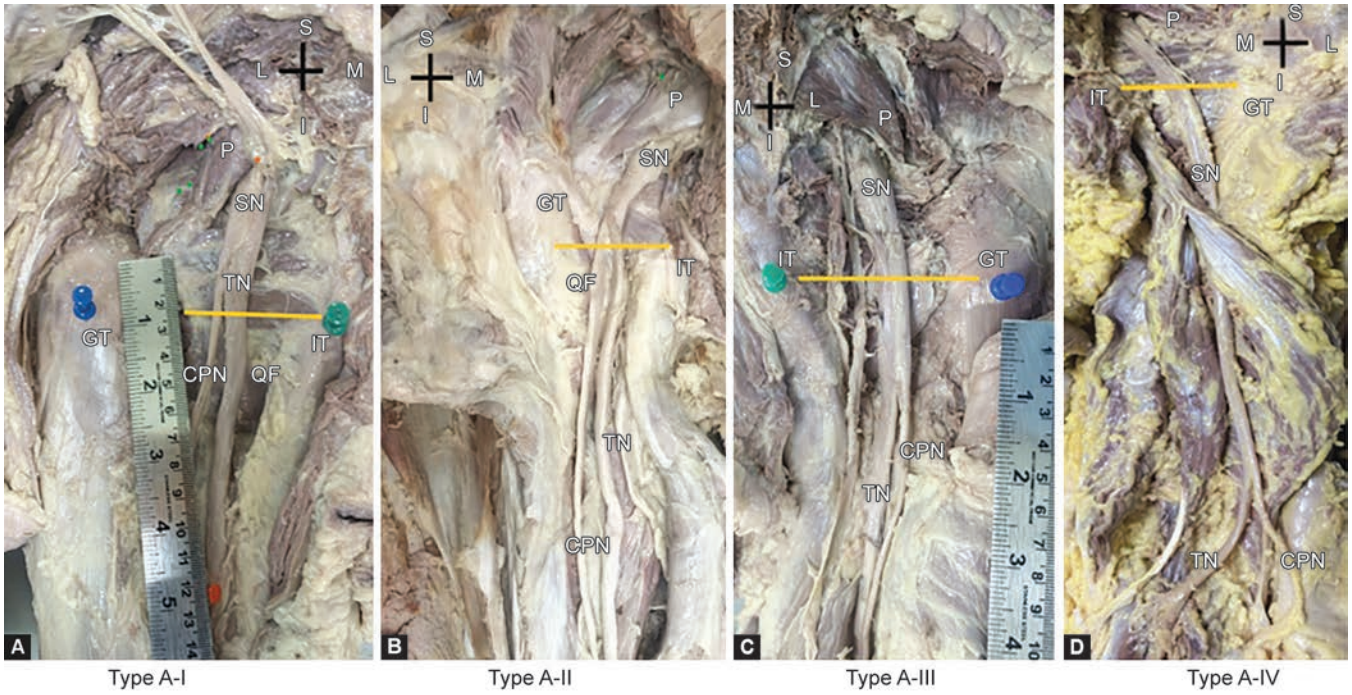

Figs 2A to D: Subtypes of type A: The SN emerges as a single trunk inferior to the lower border of the PM. (A) Type A-I; (B) Type A-II; (C) Type A-III; (D) Type A-IV. Abbreviations: CPN, common peroneal nerve; GT, greater trochanter; I, inferior; IT, ischial tuberosity; L, lateral; M, medial; QF, quadratus femoris; S, superior; TN, tibial nerve

significant, type A-III was the most frequent pattern (36.2%), followed by type A-II (17.2%), type A-IV (13.8%), and type A-I in 5.3% (Table 1). Implementation of the IT-SNBC enhanced reproducibility and improved anatomical localization of extra-pelvic SN bifurcation, supporting its potential clinical and educational utility (Fig. 2).

Discussion

The SN, first described comprehensively described by Ambroise Paré in the 16th century, has long fascinated anatomists due to its considerable variability. Early observations of its bifurcation were documented by Cruveilhier in the 19th century, and subsequent cadaveric and radiological studies have confirmed significant variation in both its course and division pattern— particularly in relation to the PM.[8–11] These anatomical variations have important clinical implications, influencing the presentation and management of conditions such as PS and affecting outcomes of hip surgeries, posterior thigh interventions, and sciatic nerve blocks.[12] In the present study, we observed notable variability in the level of SN bifurcation. The most frequent configuration identified was Beaton and Anson's type A pattern, where the undivided SN passes beneath the PM. This was observed in 72.41% of limbs, a figure lower than the global pooled prevalence of 85.2% (95% CI: 78.4–87.0) reported by Tomaszewski et al.[4] Interestingly, when compared to similar studies from other African cohorts—including Ethiopian, Kenyan, and Ugandan populations, where type A occurs in approximately 85.9% of cases—our findings suggest a comparatively higher rate of anatomical variation within the South African sample studied.[13–15]

Focusing specifically on the type A variant, we aimed to explore the extra-pelvic bifurcation patterns of the SN in greater detail. Traditionally, the SN is described as a single trunk formed by the TN and CPN, originating from the lumbosacral plexus (L4–S3) and exiting the pelvis via the greater sciatic foramen inferior to the PM.[16] However, contemporary evidence has challenged this textbook

Table 2: Clinical implications of SN variations in relation to IT

Type of SN	*Description*	*Clinical implication*
Type A-I (Above IT)	SN bifurcation proximal to the superior border of the IT	May result in incomplete anesthesia when the block is attempted at the IT level
Type A-II (At-IT)	SN bifurcation at the level of the IT	Provides a predictable and effective block site
Type A-III (Infra-IT, short thigh)	SN bifurcation 0–10 cm distal to the IT	Increased risk of selective nerve block failure
Type A-IV (Infra-IT, long thigh)	SN bifurcation >10 cm distal to the IT	Nerves may be more resilient to compression, but blocks are technically more difficult
Non-type A	High division in pelvis (sciatic–piriformis variants)	Can complicate gluteal surgeries and regional anesthesia; risk of inadvertent nerve injury

IT, ischial tuberosity; SN, sciatic nerve

depiction. Early or high bifurcation of the SN is now recognized as a common finding, with prevalence rates ranging from 16 to 60%, depending on methodology and population sampled.[17,18] We did not find any statistically significant differences in bifurcation patterns based on sex or laterality.

This trend is consistent with findings by Adibatti and Sangeetha, who noted minor sex-based variations without significant clinical impact. Nevertheless, such insights could guide further investigation into population-specific surgical risk stratification.[19] In the present study, 72.41% of dissected limbs exhibited extra-pelvic bifurcation conforming to Beaton and Anson's type A configuration. Despite being the most common type, these findings underscore a dominant presence of anatomical variation, even in grossly normal cadaveric specimens. Our data align with studies that have described high SN division in more than half of cases, including those by Issack and Helfet, which emphasize the need for clinical awareness during posterior approaches to the hip, SN blocks, and surgeries involving the hamstrings.[20–23]

A key advancement in this study is the introduction of the IT-based SNBC, which standardizes the vertical location of SN bifurcation relative to a consistent bony landmark. Ischial Tuberosity-based SNBC provides a reproducible framework for anatomical description, surgical planning, regional anesthesia, and radiological assessment. This approach resolves prior ambiguity in defining "high" vs "low" divisions, which was previously subject to arbitrary demarcation.[24] In our series, type A-III emerged as the most common subtype, seen in 36.2% of cases. By using clear anatomical landmarks and vertical reference points, this classification enhances objectivity, offering a framework suitable for anatomical education, clinical imaging interpretation, and operative planning. The clinical implications of these variations are detailed and systematically classified in Table 2.

Developmentally, SN variations arise during early formation of the lumbosacral plexus and lower limb buds. The final pathway of the nerve depends on coordinated growth and fusion of tibial (ventral) and common peroneal (dorsal) components. Delays or deviations in this process, or abnormal PM development, may result in high or aberrant bifurcation, including nerves piercing or passing above the muscle.[2,18] These anatomical variants are not pathological per se, but they have significant clinical relevance due to their association with PS, increased risk of nerve injury during procedures, and challenges in regional anesthesia. Unrecognized variations can increase the risk of iatrogenic injury during orthopedic or neurosurgical procedures, and early SN division can lead to incomplete or failed SN blocks if both branches are not individually targeted.[25] By providing a morphometrically anchored, anatomically reproducible classification, IT-SNBC supports improved procedural safety, precise imaging interpretation, and enhanced anatomical education. Additionally, standardized landmark-based morphometric indices may aid radiologists in localizing SN entrapments or variant courses more accurately during MRI assessment. This is especially valuable in distinguishing PS from lumbar radiculopathies, which often present with similar clinical features. A precise anatomical framework supports more targeted diagnostic and therapeutic interventions, reducing both diagnostic delay and procedural complications.

Limitations and Future Scope

While this study utilized formalin-fixed cadavers to ensure structural integrity and accurate measurements, the absence of correlative imaging or intraoperative validation may limit direct clinical applicability. Future research could focus on MRI- or ultrasound-based validation of the IT-SNBC in live patients, particularly in cases of SN entrapment, PS, or failed nerve blocks. Integration of IT-SNBC into 3D anatomical atlases, surgical simulation models, and virtual reality platforms could further bridge the gap between cadaveric anatomy and clinical practice. Additionally, there is scope to explore whether IT-SNBC patterns correlate with anthropometric parameters, population-specific traits, or genetic factors.

Conclusion

This study underscores the considerable anatomical variability of the SN, especially in extra-pelvic bifurcation patterns. The introduction of the IT-SNBC provides a novel, reproducible, and objective framework for categorizing these variations. By anchoring classification to a consistent bony landmark, IT-SNBC enhances anatomical localization, supports surgical planning, improves the accuracy of regional anesthesia, and aids diagnostic imaging. As population-specific anatomical variations continue to be documented, combining morphometric precision with clinical awareness is essential to optimize patient safety and procedural outcomes.

Data Availability Statement

The authors confirm that all data supporting the findings of this study are fully contained within the article and its supplementary materials.

Ethics Statement

All procedures were conducted in accordance with the ethical standards of the relevant institutional and national committees on human research and adhered to the Helsinki Declaration (1975,

as revised in 2008). Written informed consent was obtained from all body donors prior to donation. The institutional body donation program permits the use of human cadavers and tissues for educational and research purposes. In accordance with institutional policies, formal ethical approval was not required, as documented consent for anatomical study and research had been obtained from all donors.

Supplementary Materials

All the supplementary materials are available on the website www.JAS.org.

Orcid

Vandana Tiwari https://orcid.org/0000-0003-1286-5768
Navita Aggarwal https://orcid.org/0000-0002-7639-1162
Priti Chaudhary https://orcid.org/0000-0002-5869-1743

References

1. Beaton LE, Anson BJ. The relation of the sciatic nerve and of its subdivisions to the piriformis muscle. Anat Rec 1937;70(1):1–5. DOI: 10.1002/ar.1090700102.
2. Davut O, Yakup G, Sevgi B, et al. The topographical features and variations of nervus ischiadicus in human fetuses. Bratisl Lek Listy 2011;112:475–478. PMID: 21863622.
3. Robertson WJ, Kelly BT. The safe zone for hip arthroscopy: A cadaveric assessment of central, peripheral, and lateral compartment portal placement. Arthroscopy 2008;24(9):1019–1026. DOI: 10.1016/j.arthro.2008.05.008.
4. Tomaszewski KA, Graves MJ, Henry BM, et al. Surgical anatomy of the sciatic nerve: A meta-analysis. J Orthop Res 2016;34(10):1820–1827. DOI: 10.1002/jor.23186.
5. Huanmanop T, Agthong S, Chentanez V. Evaluation of the sciatic nerve location regarding its relationship to the piriformis muscle. Folia Morphol 2020;79(4):681–689. DOI: 10.5603/FM.a2019.0140.
6. Lee CS, Tsai TL. The relation of the sciatic nerve to the piriformis muscle. Taiwan Yi Xue Hui ZaZhi 1974;73(2):75–80. PMID: 4527572.
7. Natsis K, Totlis T, Konstantinidis GA, et al. Anatomical variations between the sciatic nerve and the piriformis muscle: A contribution to surgical anatomy in piriformis syndrome. Surg Radiol Anat 2014;36(3):273–280. DOI: 10.1007/s00276-013-1180-7.
8. Pećina M. Contribution to the etiological explanation of the piriformis syndrome. Cells Tissues Organs 1979;105(2):181–187. DOI: 10.1159/000145121.
9. Shrivastava T, Garg L, Mishra BK, et al. High division of sciatic nerve. Int J Res Med Sci 2014;2(2):686–688. DOI: 10.5455/2320-6012.ijrms20140559.
10. Smoll NR. Variations of the piriformis and sciatic nerve with clinical consequence: A review. Clin Anat 2010;23(1):8–17. DOI: 10.1002/ca.20893.
11. Bharadwaj UU, Varenika V, Carson W, et al. Variant sciatic nerve anatomy in relation to the piriformis muscle on magnetic resonance neurography: A potential etiology for extraspinal sciatica. Tomography 2023;9(2):475–484. DOI: 10.3390/tomography9020039.
12. Atoni AD, Oyinbo CA, Francis DAU, et al. Anatomic variation of the sciatic nerve: A study on the prevalence and bifurcation loci in relation to the piriformis and popliteal fossa. Acta Med Acad 2022;51(1):52–58. DOI: 10.5644/ama2006-124.370.
13. Valenzuela-Fuenzalida JJ, Inostroza-Wegner A, Osorio-Muñoz F, et al. The association between anatomical variants of musculoskeletal structures and nerve compressions of the lower limb: A systematic review and meta-analysis. Diagnostics (Basel). 2024;26;14(7):695. DOI: 10.3390/diagnostics14070695.
14. Kegoye ES, Ojewale AO, Ezekiel W, et al. Morphologic and morphometric bilateral analysis and sexual dimorphism in sciatic nerves of adult cadaveric specimens in Uganda. BMC Musculoskelet Disord. 2025 Apr 29;26(1):422. DOI: 10.1186/s12891-025-08641-9.
15. Ogeng'o JA, El-Busaidy H, Mwika PM, et al. Variant anatomy of sciatic nerve in a black Kenyan population. Folia Morphol (Warsz) 2011;70(3):175–179. PMID: 21866528.
16. Moore KL, Dalley AF, Agur AMR. Clinically oriented anatomy. 8th ed. Wolters Kluwer; 2018.
17. Haładaj R, Pingot M, Polguj M, et al. Anthropometric study of the piriformis muscle and sciatic nerve: A morphological analysis in a Polish population. Med Sci Monit 2015;21:3760–3768. DOI: 10.12659/msm.894353.
18. Ugrenović S, Jovanović I, Krstić V, et al. The level of the sciatic nerve division and its relations to the piriform muscle. Vojnosanit Pregl 2005;62(1):45–49. DOI: 10.2298/vsp0501045u.
19. Adibatti M, Sangeetha V. Study on variant anatomy of sciatic nerve. J Clin Diagn Res 2014;8(8):AC07–AC09. DOI: 10.7860/JCDR/2014/9116.4725.
20. Issack PS, Helfet DL. Sciatic nerve injury associated with acetabular fractures. HSS J. 2009;5(1):12–18. DOI: 10.1007/s11420-008-9099-y.
21. Prakash, Bhardwaj AK, Devi MN, et al. Sciatic nerve division: A cadaver study in the Indian population and review of the literature. Singapore Med J 2010;51(9):721–723. PMID: 20938613.
22. Bergsteedt BJ, Cilliers K, Greyling LM. Bifurcation of the sciatic nerve: A descriptive study on a South African cadaver cohort. Morphologie. 2022;106(354):155–162. DOI: 10.1016/j.morpho.2021.05.002.
23. Grewal H, Singla RK, Singh R, et al. Different levels of bifurcation of sciatic nerve: a novel classification based on a cadaveric study in Indian population. Int J Anat Res 2016;4(3):2743–2749. DOI: 10.16965/ijar.2016.323.
24. Pokorný D, Jahoda D, Veigl D, et al. Topographic variations of the relationship of the sciatic nerve and the piriformis muscle and its relevance to palsy after total hip arthroplasty. Surg Radiol Anat 2006;28(1):88–91. DOI: 10.1007/s00276-005-0056-x.
25. Karmakar MK, Shariat AN, Pangthipampai P, et al. High-definition ultrasound imaging defines the paraneural sheath and the fascial compartments surrounding the sciatic nerve at the popliteal fossa. Reg Anesth Pain Med. 2013;38(5):447–451. DOI: 10.1097/AAP.0b013e31829ffcb4.

ORIGINAL RESEARCH

Comparative Study of Microscopic Changes in Human Placenta of Pre-eclamptic and Eclamptic Patients of Eastern Uttar Pradesh

Arpana Srivastava[1], Bindu Singh[2], Yogendra Singh[3], Shilpa Singh[4], Soumya Agrawal[5], Rahul Singh[6] Isha Ragini[7]

Received on: 12 December 2025; *Accepted on:* 02 January 2026; *Published on:* 20 January 2026

Abstract

Introduction: Pregnancy-induced hypertension (PIH) is a major cause of maternal and perinatal morbidity worldwide and is known to significantly alter placental structure and function. These alterations impair uteroplacental perfusion and contribute to adverse outcomes such as intrauterine growth restriction, preterm birth, and stillbirth. Understanding the microscopic changes in the placenta associated with pre-eclampsia (PE) and eclampsia is essential for better insight into disease progression.

Aim and objectives: To evaluate and compare the microscopic changes in placentas from normotensive pregnancies and those complicated by PIH (PE and eclampsia).

Methodology: This comparative study was conducted in the Anatomy Department and Obstetrics and Gynecology Department at BRD Medical College, Gorakhpur. A total of 100 placentas were examined: 50 normal, 26 pre-eclamptic, and 24 eclamptic. All samples were collected immediately after delivery, fixed in 10% neutral buffered formalin, processed routinely, and stained with hematoxylin and eosin. Histopathological parameters were graded using standard scoring criteria and analyzed statistically using the Chi-square test.

Results: All six histological parameters showed statistically significant associations and demonstrated progressively worsening lesions from normal to PE and eclampsia. Fibrin deposition increased from 0% in normal cases to 58% severe in eclampsia; fibrinoid necrosis from 0 to 96%; syncytial knots from 22 to 46% severe; cytotrophoblastic proliferation from 6 to 42% severe; endothelial proliferation from 0 to 71% severe; and calcification from 48 to 69%.

Conclusion: Pregnancy-induced hypertension is strongly linked with progressive and characteristic placental histopathological alterations. The severity of microscopic changes increased from normal to PE and was most pronounced in eclampsia, reflecting worsening placental hypoxia and vascular injury. These findings highlight the value of placental evaluation in understanding disease severity and predicting fetal outcomes.

Keywords: Eclampsia, Histology, Placenta, Pre-eclampsia, Pregnancy-induced hypertension.

Journal of Anatomical Sciences (2025): 10.5005/jas-11049-0013

Introduction

The placenta is a crucial organ that supports pregnancy by enabling the transfer of nutrients, gases, and metabolic wastes between the mother and the developing fetus. Its structural integrity and functional efficiency are essential for normal fetal growth. In pregnancy-induced hypertension (PIH), these physiological processes become disrupted due to compromised placental perfusion, ultimately predisposing both mother and fetus to significant complications. Understanding the morphological and histopathological changes associated with PIH is therefore vital for elucidating its pathogenesis and strengthening clinical management.[1,2]

According to the World Health Organization (2021), approximately 10% of all pregnancies are complicated by hypertension, contributing to nearly 14% of global maternal mortality.[3] Pre-eclampsia (PE) and eclampsia result in approximately 5,00,000 perinatal deaths and 70,000 maternal deaths each year, with the heaviest burden in South Asia and Sub-Saharan Africa. In India, PIH accounts for nearly 5–10% of pregnancies and is a major cause of maternal mortality, particularly in regions with limited antenatal services and constrained healthcare resources.[3]

Pregnancy-induced hypertension includes several hypertensive conditions such as gestational hypertension, PE, eclampsia, and chronic hypertension with superimposed PE. Pre-eclampsia is a pregnancy-specific, multisystem disorder that arises after 20 weeks of gestation and is characterized by newly elevated blood pressure (systolic ≥140 mm Hg and/or diastolic ≥90 mm Hg) accompanied by proteinuria or evidence of systemic organ involvement. Eclampsia represents its most severe form, manifested by new-onset generalized tonic–clonic seizures not attributable to other neurological causes. These complications stem from widespread endothelial dysfunction, leading to impaired placental circulation and systemic involvement of organs such as the liver, kidneys, brain, and coagulation pathways.[1,2]

[1–7]Department of Anatomy, Baba Raghav Das Medical College, Gorakhpur, Uttar Pradesh, India

Corresponding Author: Arpana Srivastava, Department of Anatomy, Baba Raghav Das Medical College, Gorakhpur, Uttar Pradesh, India, Phone: +91 7704077640, e-mail: arpanasri007@gmail.com

How to cite this article: Srivastava A, Singh B, Singh Y, *et al*. Comparative Study of Microscopic Changes in Human Placenta of Pre-eclamptic and Eclamptic Patients of Eastern Uttar Pradesh. J Anat Sciences 2025;33(2):51–57.

Source of support: Nil

Conflict of interest: None

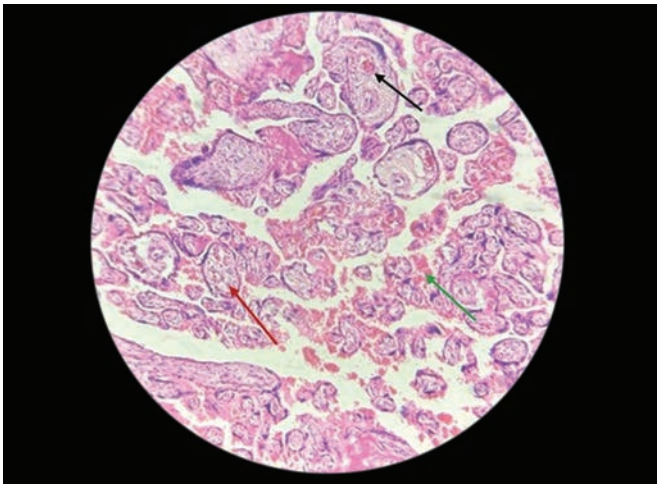

Fig. 1: Showing the appearance of chorionic villi in a normal placenta. Red arrow (chorionic villi having an inner core of cytotrophoblast with fetal blood vessels), black arrow (fetal blood vessels), green arrow (maternal blood between intervillous spaces) at 100× magnification

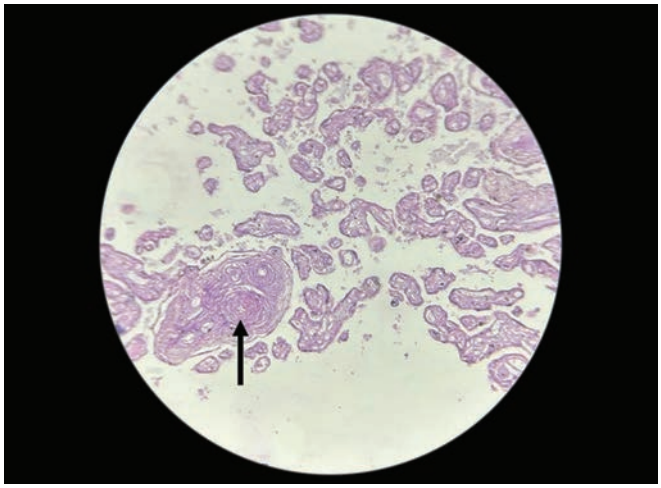

Fig. 2: Showing fibrin deposition and hyalinization (mild) in chorionic villi of PE patients at 100× magnification

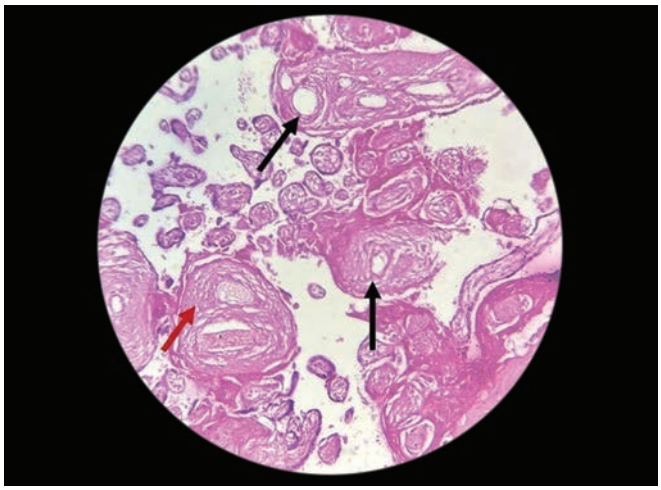

Fig. 3: Showing fibrin deposition and hyalinization with red arrow (severe) and endothelial proliferation with black arrow (severe) in chorionic villi of eclampsia patients at 100× magnification

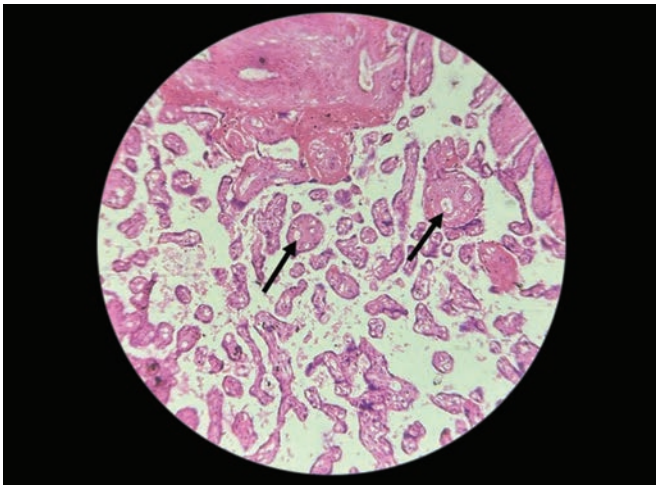

Fig. 4: Showing endothelial proliferation (mild) in the chorionic villi of PE patients at 100× magnification

The resulting maternal and perinatal consequences include intrauterine growth restriction, preterm delivery, placental abruption, and multi-organ compromise. Despite the clinical significance of PIH, region-specific data—particularly from Eastern UP—remain limited, thus essential for generating locally relevant evidence that can support improved preventive and therapeutic strategies.

A mature placenta is a discoid organ weighing 400–600 gm and measuring approximately 15 cm in diameter. It performs specialized functions, while the chorionic villi—composed of syncytiotrophoblast and cytotrophoblast layers—serve as the main site of maternal–fetal exchange. In PIH, insufficient remodeling of the spiral arteries leads to reduced uteroplacental blood flow, resulting in a smaller, ischemic placenta. Chronic hypoxia triggers oxidative stress and endothelial damage, further compromising placental function.[1,2] Histologically, PIH-affected placentas commonly exhibit villous infarction, fibrinoid necrosis, excessive fibrin deposition, thickened vessel walls, thrombosis, and an increased number of syncytial knots. These features reflect ongoing hypoxic and degenerative processes that impair nutrient and oxygen transfer to the fetus. Consequently, the risk of outcomes such as growth restriction, preterm birth, and—in severe cases—stillbirth increases (Figs 1 to 5).

Aim and Objectives

Aim

To assess and compare the microscopic changes in placental tissue from women with PIH—including PE and eclampsia—with those from normotensive pregnancies, and to examine how these histopathological alterations relate to fetal outcomes.

Objectives

To analyze and compare placental histological features such as fibrinoid necrosis, fibrin deposition, villous calcification, syncytial knot formation, cytotrophoblastic cellular proliferation, and endothelial changes across normotensive, pre-eclamptic, and eclamptic groups.

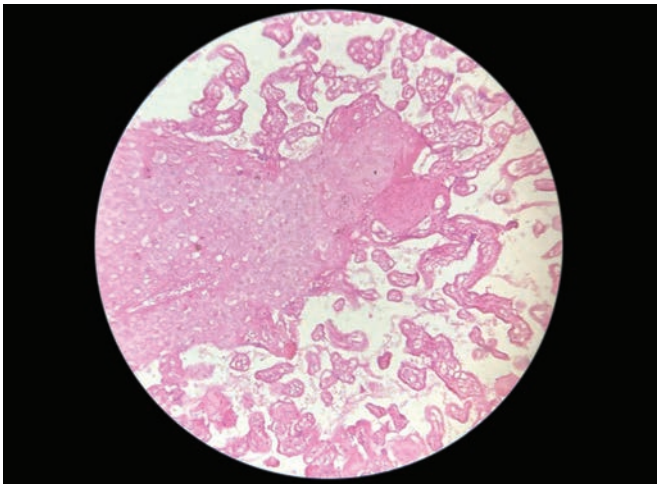

Fig. 5: Showing fibrinoid necrosis in the chorionic villi of eclampsia patients at 100× magnification

Methodology

This comparative study was done in the Anatomy Department, and placentae were collected from the OBG Department of Baba Raghav Das Medical College, Gorakhpur. Ethical approval was obtained from the institutional ethical committee (IEC) of BRD Medical College.

Inclusion Criteria

- Placentas from normotensive, pre-eclamptic, and eclamptic pregnancies between 37 and 40 weeks of gestation.
- Mothers who provided informed and voluntary consent for participation.

Exclusion Criteria

- Pregnancies associated with metabolic or endocrine disorders such as diabetes mellitus, gestational diabetes, or hypothyroidism.
- Cases positive for viral infections.
- Women with pre-existing chronic hypertension or hypertension secondary to other medical conditions.

Placentas and their umbilical cords were collected immediately following delivery in the Department of Obstetrics and Gynecology. Samples were taken from both primigravida and multigravida women belonging to the normotensive, pre-eclamptic, and eclamptic pregnancies. The attached membrane and cord were cut from 10 cm of their attachment, and each placenta was rinsed thoroughly under tap water.

The specimens were fixed in 10% formalin for a minimum of 1 week. From each placenta, tissue samples measuring about 1 cm^3 were obtained from the maternal surface. Tissues were processed using ascending grades of alcohol (dehydration), followed by clearing in alcohol–xylene mixtures and subsequent embedding in paraffin wax to prepare tissue blocks.[4]

Sections of 7–10 µm thickness were taken with a semi-automatic microtome. The sections were placed on a hot water bath (55°C) and mounted on slides coated with albumin. Slides were air-dried and stained with H&E stain.[5,6]

Stained sections were examined at 100× magnification, and the microscopic findings were documented in detail, as summarized in Table 1.

Table 1: Histopathological scoring[4]

Fibrin deposition	
Absent	Absent
Mild	Present < 25%/lpf
Moderate	Present = 25–50%/lpf
Severe	Present > 50%/lpf
Fibrinoid necrosis	
Absent	Absent
Mild	Present
Syncytial knots	
Absent	Absent
Mild	Present < 25%/lpf
Moderate	Present = 25–50%/lpf
Severe	Present > 50%/lpf
Cytotrophoblastic cellular proliferation	
Absent	Absent
Mild	Present <25%/lpf
Moderate	Present = 25–50%/lpf
Severe	Present > 50%/lpf
Endothelial proliferation	
Absent	Absent
Mild	Present <25%/lpf
Moderate	Present = 25–50%/lpf
Severe	Present > 50%/lpf
Calcification	
Absent	Absent
Mild	Present

Observations and Results

The histopathological evaluation of 100 placentas comprising normal pregnancies ($n = 50$), PE ($n = 26$), and eclampsia ($n = 24$) revealed a strong and statistically significant association between PIH and all major histopathological parameters assessed, as given in Table 2 and Figures 6 to 11. Fibrin deposition demonstrated a highly significant relationship with PIH ($\chi^2 = 85.091$, df = 6, $p < 0.001$). While 76% of normal placentas had no deposition, all pre-eclamptic and eclamptic placentas exhibited some degree of fibrin accumulation, with severe deposition predominantly seen in eclampsia (58%). Fibrinoid necrosis also showed a strong, significant association with hypertensive disorders ($\chi^2 = 63.370$, df = 2, $p < 0.001$). It was absent in all normal placentas but increased markedly in PE (42%) and was almost universal in eclampsia (96%).

A similar trend was observed with syncytial knots, which were significantly associated with PIH ($\chi^2 = 67.102$, df = 4, $p < 0.001$). Most normal cases (78%) showed no knot formation, whereas pre-eclamptic placentas showed predominantly mild to moderate grades, and eclamptic placentas displayed markedly higher grades, with 46% showing severe knots. Cytotrophoblastic cellular proliferation demonstrated one of the strongest associations ($\chi^2 = 106.846$, df = 6, $p < 0.001$). Almost all normal placentas showed no proliferation (94%), while all hypertensive placentas displayed increasing grades of hyperplasia. Severe proliferation was most prominent in eclampsia (42%).

Table 2: Frequency distribution of histological parameters in normal, PE, and eclamptic patients

Histological parameters	*Grading*	*Normal (n = 50)*	*PE (n = 26)*	*Eclampsia (n = 24)*
Fibrin deposition	Absent	38	0	0
	Mild	12	7	4
	Moderate	0	10	6
	Severe	0	9	14
Fibrinoid necrosis	Absent	50	15	1
	Mild	0	11	23
Syncytial knots	Absent	39	10	0
	Mild	11	9	4
	Moderate	0	7	9
	Severe	0	0	11
Cytotrophoblastic cellular proliferation	Absent	47	0	0
	Mild	3	12	5
	Moderate	0	8	9
	Severe	0	6	10
Endothelial proliferation	Absent	50	6	0
	Mild	0	5	2
	Moderate	0	9	5
	Severe	0	6	17
Calcified villous spots	Absent	24	8	8
	Mild	26	18	16

PE, pre-eclampsia

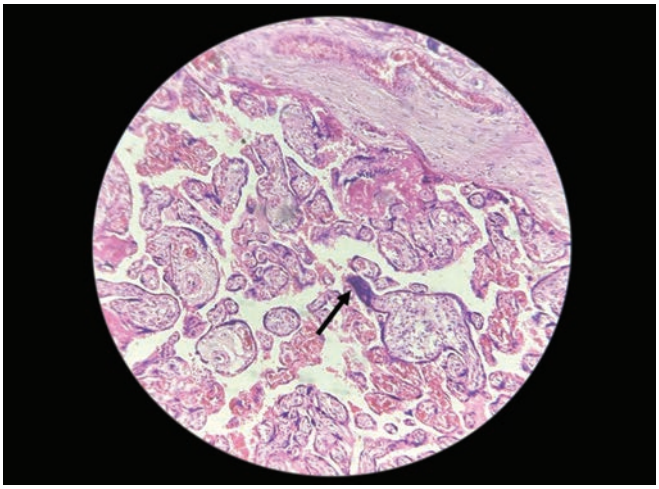

Fig. 6: Showing syncytial knots (mild) in the chorionic villi of normal pregnancies at 100× magnification

Endothelial proliferation also showed a highly significant association with PIH ($\chi^2 = 119.471$, df = 6, $p < 0.001$). None of the normal placentas exhibited endothelial proliferation, whereas all hypertensive cases showed varying degrees, with severe proliferation most frequent in eclampsia (71%). Calcified villous spots displayed a statistically significant relationship with PIH as well ($\chi^2 = 7.585$, df = 2, $p = 0.023$). Calcification was present in nearly half of the normal placentas (48%) but increased in PE (69%) and eclampsia (67%).

All histological parameters exhibited significant differences across the three study groups, with increasing severity of changes

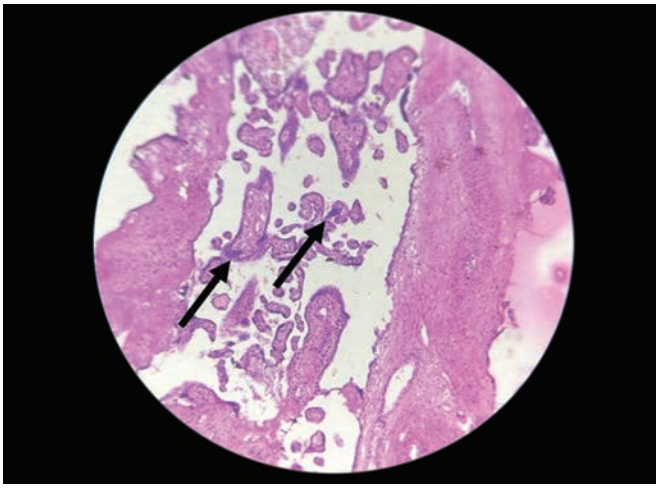

Fig. 7: Showing syncytial knots (severe) in the chorionic villi of eclampsia patients at 100× magnification

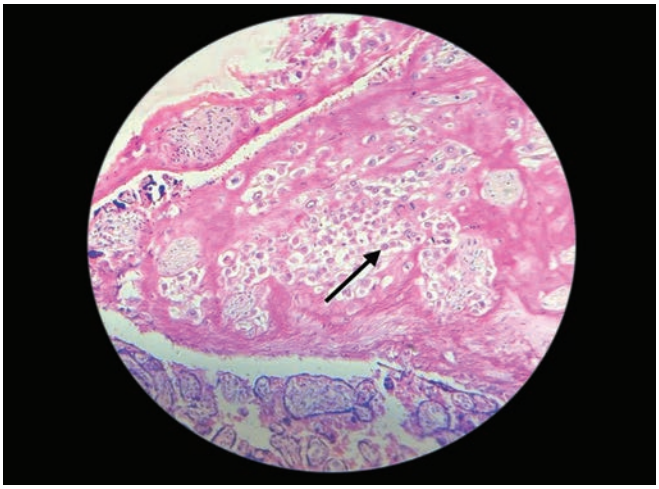

Fig. 8: Showing cytotrophoblastic proliferation (severe) in the chorionic villi of eclampsia patients at 100× magnification

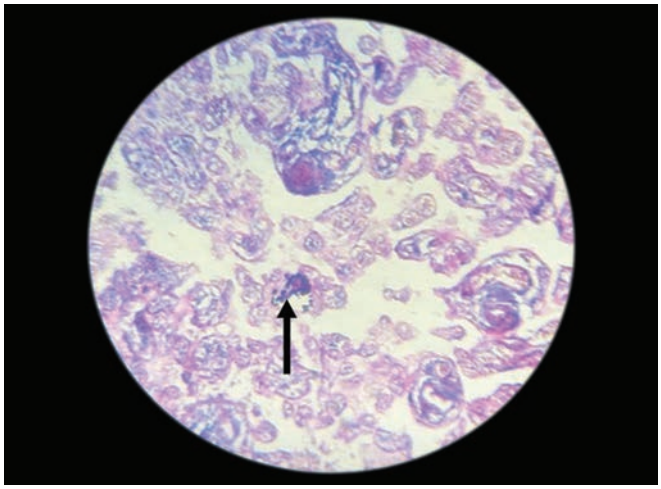

Fig. 9: Showing calcified spots in the chorionic villi of eclampsia patients at 100× magnification

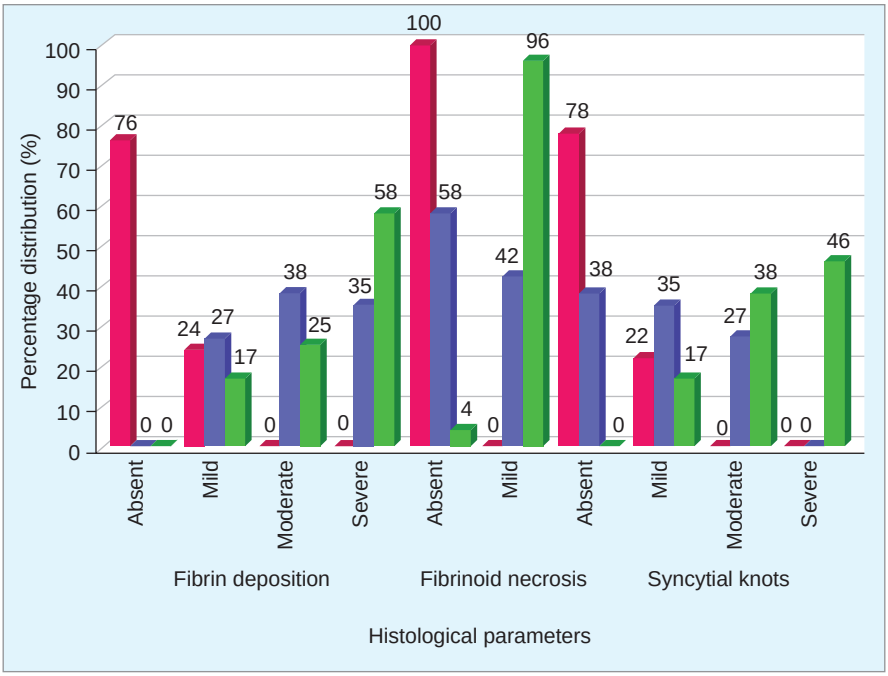

Fig. 10: Showing the percentage distribution of histological parameters (fibrin deposition, fibrinoid necrosis, and syncytial knots) in normal, PE, and eclampsia patients

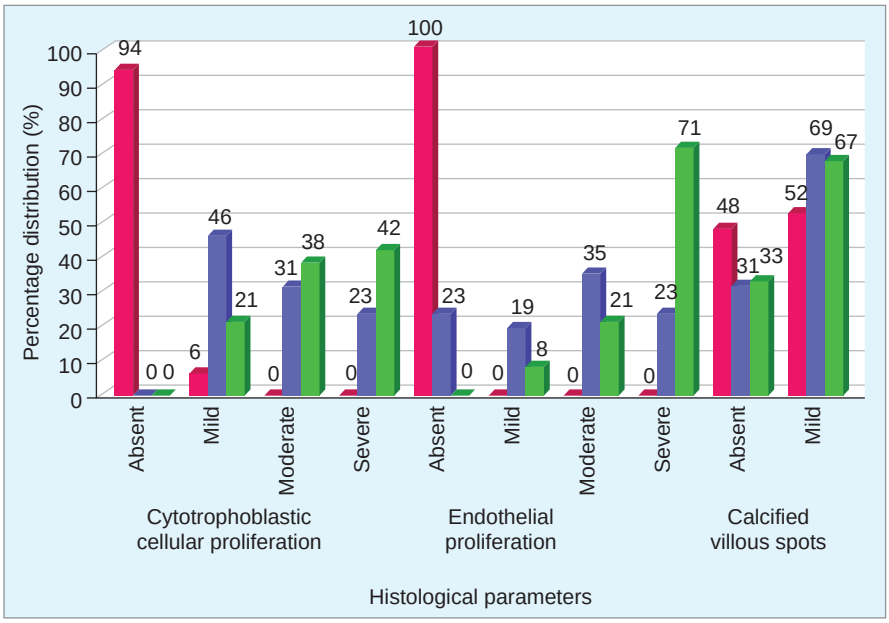

Fig. 11: Showing the percentage distribution of histological parameters (cytotrophoblastic cellular proliferation, endothelial proliferation, and calcified villous spots) in normal, PE, and eclampsia patients

from normal to PE and most prominently in eclampsia. The consistently significant Chi-square values and *p*-values reinforce that hypertensive disorders of pregnancy are strongly associated with characteristic and progressively worsening placental histopathological alterations with its increasing severity.

Discussion

The present study highlights a clear and progressive increase in placental histopathological alterations across normal pregnancies, PE, and eclampsia as compared with previously published studies, which is collectively shown in Table 3.

In our study, fibrin deposition increased markedly from normal to pre-eclamptic and eclamptic placentas, with severe deposition most common in eclampsia (58%). These findings closely resemble those of Vasantha Malini et al., who also reported significantly higher fibrin accumulation in PE compared to controls ($p < 0.001$).[7] Similarly, Deepak Donthi et al. observed a higher frequency of intravillous and perivillous fibrin in hypertensive

Table 3: Comparison of histological parameters in normal, PE, and eclamptic patients across different studies

Parameter	*Bhawana Sahay et al., 2016*[9]	*G. Ratna and Karunavathi G 2016*[10]	*Donthi et al., 2020*[8]	*Vasantha Malini et al., 2024*[7]	*Present study*
Fibrin deposition	Increased in PE vs controls	Higher in the PE group	Increased intravillous/ perivillous fibrin 94% in PE and 90% in eclampsia	Significantly higher in PE ($p < 0.001$)	Progressive rise; severe 58% in eclampsia
Fibrinoid necrosis	Significant rise in PE (more cases >10%)	Increased necrosis in PE	Strongly increased in PE/E groups	Noted frequently in PE cases	0% (normal), 42% (PE), 96% (E)
Syncytial knots	Higher frequency in PE	60% in PE vs 20% controls	Increased 73.3% in PE and 75% in eclampsia	Markedly higher in PE	0–78% (normal), rising to 46% severe in E
Cytotrophoblastic hyperplasia	Higher proliferation (>40%) in PE	50% in PE vs 6.6% controls	Noted increased trophoblastic reaction	Moderate rise in PE	6% (normal) vs 100% (PE/E)
Endothelial proliferation/ Vascular changes	Moderate increase	Increased vascular pathology in PE placentas	Thickened/hyalinized membranes 105 in PE and 60% in eclampsia	Increase in PE	Absent in normal, severe in 71% of E
Calcification	—	40% in cases vs 16% controls	Focal/diffuse increase 76.7% in PE and 80% in eclampsia	22% (N) vs 52% (PE)	48% (N), 69% (PE), 67% (E)

E, eclampsia; PE, pre-eclampsia

placentas, confirming fibrin accumulation as a robust indicator of uteroplacental insufficiency.[8]

Fibrinoid necrosis in the present study was absent in all normal placentas but increased sharply in PE (42%) and dramatically in eclampsia (96%). This aligns with findings from Bhawana Sahay et al., who reported that more than 60% of hypertensive placentas showed moderate to severe fibrinoid necrosis.[9] The similarity in results across studies supports the interpretation that fibrinoid change is one of the earliest and most reliable indicators of villous injury due to chronic ischemia.

Syncytial knots, a marker of accelerated villous maturation, also increased progressively with disease severity in the present study. These results closely match those of Ratna G and Karunavathi G who documented significantly higher syncytial knot formation in PE (60%) compared to controls (20%).[10] The findings also correlate with Donthi et al., who demonstrated increased syncytial knotting in both PE and eclampsia groups, indicating heightened oxidative stress.[8]

Cytotrophoblastic cellular hyperplasia was another parameter showing strong agreement across studies. In our study, only 6% of normal placentas showed proliferation, while 100% of hypertensive placentas demonstrated hyperplasia of varying grades. Bhawana Sahay et al. similarly reported that severe hyperplasia (>40%) was predominantly confined to PE cases, supporting the theory of trophoblastic compensatory response to reduced perfusion.[9] Ratna and Karunavathi also observed significantly elevated cytotrophoblastic hyperplasia in cases compared to controls (50 vs 6.66%), echoing our findings.[10]

Endothelial proliferation, though absent in all normal placentas in the present study, was increasingly noted in PE and maximally in eclampsia (71% severe). This trend strongly correlates with Donthi et al., who also documented progressive thickening, hyalinization, and vascular remodeling in hypertensive placentas, further validating endothelial proliferation as a hallmark of severe disease.[8]

Calcified villous spots were present in almost half of the controls (48%) in our study but increased significantly in hypertensive groups (69% in PE and 67% in eclampsia). This moderately elevated pattern is comparable to Vasantha Malini et al., who reported higher calcification in PE (52%) compared to controls (22%).[7] The present findings thus support existing evidence that hypertensive disorders lead to premature villous aging.

All the comparative studies consistently demonstrate that PE and eclampsia produce characteristic placental lesions related to hypoxia, oxidative stress, defective trophoblastic invasion, and altered uteroplacental blood flow. The present study is in strong agreement with these authors, strengthening the conclusion that placental histopathology is an essential tool for assessing disease severity and predicting adverse fetal outcomes.

Conclusion

The study demonstrated a clear and progressive association between PIH and a range of placental histopathological alterations. All assessed histological parameters varied significantly across normal, pre-eclamptic, and eclamptic placentas. Normal pregnancies showed minimal or absent pathological changes, whereas PE exhibited moderate abnormalities, and eclampsia showed the most severe grades in nearly every category. The marked increase in fibrin accumulation, necrosis, trophoblastic proliferation, and endothelial changes reflected escalating placental hypoxia and vascular injury with advancing disease severity. Higher calcification rates in hypertensive groups further indicated premature villous aging. The consistently significant Chi-square findings confirmed that PIH markedly disrupted placental structure and function, worsening with maternal hypertension, which likely contributed to adverse maternal and fetal outcomes.

References

1. Cunningham FG. Williams obstetrics. 26th ed. McGraw Hill Medical; 2022. pp. 82–120. Available from: https://accessmedicine.mhmedical.com/book.aspx?bookid=2977#249763085.
2. Konar H. Dc Dutta's textbook of obstetrics including perinatology & contraception. 10th ed. Jaypee Brothers Medical Publishers; 2022. DOI: 10.5005/jp/books/12044.
3. World Health Organization. World health statistics 2021: Monitoring health for the SDGs, sustainable development goals. 2021 [cited

2025 Jun 26]. Available from: https://www.who.int/publications/i/item/9789240027053.
4. Srivastava A, Sinan B, Sinan Y, et al. Microscopic studies or human placenta in pregnancy induced hypertensive patients. Int J Acad Med Pharm 2025;7(4);319–324. DOI: 10.47009/jamp.2025.7.4.60.
5. Suvarna KS, Layton C, Bancroft JD, et al. Bancroft's theory and practice of histological techniques. 8th ed. Elsevier; 2018. DOI: 10.1016/C2015-0-00143-5.
6. Pushpalatha K, DB. Inderbir Singh's textbook of human histology. 10th ed. Jaypee Brothers Medical Publishers; 2022.
7. Malini MV, Sivaprasad GV, Teki S. A study on the histopathological changes in the placenta of pre-eclampsia mothers. International Journal of Pharmaceutical and Clinical Research. 2024;16(8):739–744. Available from: www.ijpcr.com.
8. Donthi D, Malik P, Mohamed A, et al. An objective histopathological scoring system for placental pathology in pre-eclampsia and eclampsia. Cureus 2020;12(10):e11104. DOI: 10.7759/cureus.11104.
9. Sahay B, Talukdar L, Sahay P, et al. Comparative study between histological changes in placenta from pre-eclampsia cases and normal pregnancy with special reference to cytotrophoblastic cell hyperplasia, villous stromal fibrosis and fibrinoid necrosis. Int J Res Med Sci 2016:4884–4888. DOI: 10.18203/2320-6012.ijrms20163785.
10. Ratna G, Karunavathi G. A comparative study of the pathological changes in placenta of pre-eclamptic patients and its relation to foetal outcome. IOSR Journal of Dental and Medical Sciences 2016;15(2):5–7. Available from: www.iosrjournals.org.

ORIGINAL RESEARCH

Comparative Morphometric Analysis of the Hypoglossal Canal across Ethnic Groups: Data from Eastern Uttar Pradesh and Global Literature

Prasenjit Bose[1], Anuj K Maurya[2], Raj Kumar[3], Barkha Singh[4]

Received on: 12 December 2025; *Accepted on:* 03 January 2026; *Published on:* 20 January 2026

Abstract

Introduction: The hypoglossal canal (HC) is a key skull base conduit transmitting the hypoglossal nerve and associated neurovascular structures, with a morphology that varies considerably across populations and has important implications for craniovertebral junction surgery. This osteological study aimed to characterize HC morphometry and morphological variants in an Eastern Uttar Pradesh population and to compare these findings with international data.

Materials and methods: Twenty adult dry skulls of regional origin were examined using a digital Vernier caliper to record maximum transverse and vertical diameters of the intracranial HC opening, and the distance from the HC to the basion, bilaterally. Canal shape was classified as round, oval horizontal, or oval vertical, and anatomical variants such as accessory canals and septation were documented.

Results: Mean transverse and vertical diameters, and HC–basion distances demonstrated no statistically significant right–left differences, indicating bilateral symmetry, although individual asymmetry was present. Overall dimensions were smaller than values reported in Turkish, Italian, Egyptian, and some Indian series, supporting population-specific baseline metrics. Oval horizontal canals predominated on both sides, and accessory HCs were observed in a minority of skulls.

Conclusion: These findings provide region-specific morphometric benchmarks and highlight the variability and potential surgical risk associated with HC anatomy. Accurate knowledge of HC dimensions, shape distribution, and variant patterns in this population can inform safer planning of transcondylar and related skull base approaches and enrich comparative cranial anthropology.

Keywords: Accessory canal, Craniovertebral junction, Hypoglossal canal, Skull base, Morphometry, Transcondylar approach.

Journal of Anatomical Sciences (2025): 10.5005/jas-11049-0012

Introduction

The hypoglossal canal (HC), also known as the anterior condylar canal, is an essential anatomical conduit at the skull base transmitting critical neurovascular structures.[1–3] This bilateral bony passage extends from the posterior cranial fossa to the nasopharyngeal carotid space, coursing through the occipital bone in close proximity to the occipital condyle (OC).[1,4,5] The canal transmits the hypoglossal nerve (cranial nerve XII), the venous plexus communicating between the basilar and marginal venous systems, a meningeal branch of the ascending pharyngeal artery, and an emissary vein draining to the transverse sinus.[1–3,6]

The hypoglossal nerve innervates all intrinsic and extrinsic muscles of the tongue except the palatoglossal muscle, making it fundamental in physiological functions including phonation, deglutition, and articulation.[2,7] From an evolutionary perspective, the canal's morphology has been studied to understand the development of human vocal abilities, with larger canals hypothetically associated with enhanced speech capabilities in hominids compared to primates.[2,7]

Substantial morphometric variation exists in HC dimensions and morphology across and within populations, including transverse and vertical diameters, distances from bony landmarks, canal length, shape characteristics (oval horizontal, oval vertical, or round), and various anatomical variants such as single, double (bipartite), incomplete septation, complete septation, and accessory canals.[1,3–5,8] These variations carry significant clinical implications: In transcondylar surgical approaches to the craniovertebral junction, detailed knowledge of HC morphometry is essential to avoid hypoglossal nerve compression or injury during drilling of the OC and jugular tubercle.[3–5]

Race- and population-specific morphometric data have been reported from Turkish, Italian, Indian, Greek, Egyptian, Iranian, and Japanese populations.[1,4–8] However, contemporary morphometric data on Eastern Uttar Pradesh populations remain limited. The present study provides a detailed morphometric and morphological analysis of the HC in a sample of adult dry skulls from this region, establishing baseline values and variation patterns for regional populations while comparing findings with published international literature.

[1,2,4]Department of Anatomy, Institute of Medical Sciences, Banaras Hindu University, Varanasi, Uttar Pradesh, India

[3]Department of Anatomy, Institute of Medical Sciences, Atkot, Gujarat, India

Corresponding Author: Prasenjit Bose, Department of Anatomy, Institute of Medical Sciences, Banaras Hindu University, Varanasi, Uttar Pradesh, India, Phone: +91 9026059250, e-mail: prasenjitbose@bhu.ac.in

How to cite this article: Bose P, Maurya AK, Kumar R, *et al*. Comparative Morphometric Analysis of the Hypoglossal Canal across Ethnic Groups: Data from Eastern Uttar Pradesh and Global Literature. J Anat Sciences 2025;33(2):58–63.

Source of support: Nil

Conflict of interest: None

Materials and Methods

Sample Collection and Inclusion Criteria

Twenty adult human skulls of unknown sex were obtained from the Department of Anatomy, Institute of Medical Sciences (IMS), Banaras Hindu University, Varanasi. All specimens were from the Eastern Uttar Pradesh region. Skulls with deformities or damage affecting the foramen magnum, OCs, or HCs were excluded to ensure measurement integrity. No skulls had undergone surgical procedures.

Measurement Protocols

All linear measurements were performed using a digital Vernier caliper with a measurement accuracy of 0.01 mm. As illustrated in Figure 1, the described measurements were performed on both sides of every specimen. Parameters recorded for each HC included:

- Maximum transverse diameter (mm) – Greatest mediolateral dimension of the canal opening.
- Maximum vertical diameter (mm) – Greatest superoinferior dimension of the canal opening.
- Maximum linear distance from canal to basion (mm) – Horizontal distance from the intracranial opening of the HC to the basion (anteriormost point of the foramen magnum).
- Qualitative shape classification – Categorical assessment of canal morphology.

All measurement procedures and definitions matched established protocols from prior international studies to ensure comparability with published data.[1,3–5]

Canal Shape Classification

Canal morphology was classified into three categories based on diameter relationships:

1. Round: The difference between transverse and vertical diameter less than 0.2 mm.
2. Oval horizontal: The transverse diameter greater than vertical diameter.
3. Oval vertical: The vertical diameter greater than transverse diameter.

Statistical Analysis

Descriptive statistics including means, standard deviations, and 95% confidence intervals (CIs) were calculated for all metric parameters. Bilateral comparisons (right vs left sides) employed paired *t*-tests, with statistical significance set at $p < 0.05$. Frequency distributions were tabulated for qualitative variables including canal shape categories and anatomical variants. Comparative analysis with published data from other ethnic groups was performed to contextualize findings.

Results

Dimensional Findings

Morphometric data for the right and left HCs are summarized in Table 1 and illustrated in Figure 2. The mean maximum transverse diameter on the right side was 3.71 ± 0.56 mm (95% CI: 3.42–3.99 mm), while the left side measured 3.54 ± 0.56 mm (95% CI: 3.24–3.84 mm). The mean maximum vertical diameter on the right side was 3.59 ± 0.60 mm (95% CI: 3.28–3.90 mm), and on the left side was 3.38 ± 0.59 mm (95% CI: 3.06–3.69 mm). The mean distance from the intracranial opening of the HC to the basion was 27.66 ± 1.60 mm on the right (95% CI: 26.83–28.48 mm) and 26.91 ± 1.02 mm on the left (95% CI: 26.35–27.48 mm).

Bilateral Symmetry Analysis

No statistically significant differences were identified between the right and left sides for any measured parameter: Maximum transverse diameter ($p = 0.40$), maximum vertical diameter ($p = 0.47$), and distance from basion ($p = 0.64$). These findings

Fig. 1: Schematic illustration showing bilateral HC measurements: (1) Transverse diameter, (2) vertical diameter, and (3) distance from canal to basion (in mm)

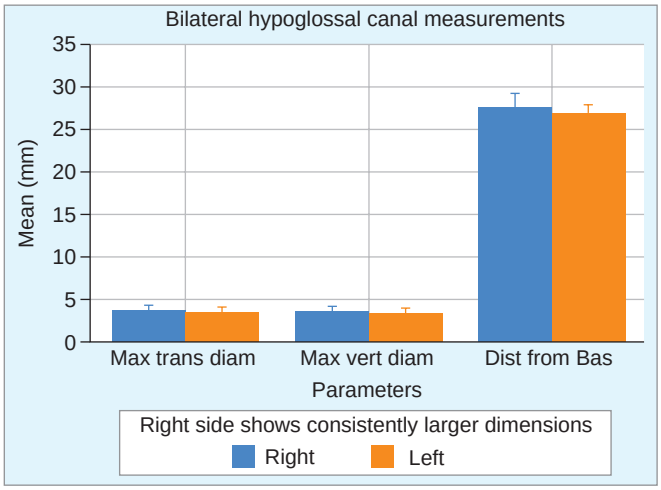

Fig. 2: Mean morphometric values (mm) for right and left HCs, presented as mean ± SD with 95% confidence intervals for key measurements: Transverse diameter, vertical diameter, and HC-to-basion distance

Table 1: Morphometric measurements of HC in Eastern Uttar Pradesh population

Parameter	*Mean (right)*	*SD (right)*	*Mean (left)*	*SD (left)*	*95% CI right*	*95% CI left*
Max transverse diameter (mm)	3.71	0.56	3.54	0.56	3.42–3.99	3.24–3.84
Max vertical diameter (mm)	3.59	0.60	3.38	0.59	3.28–3.90	3.06–3.69
Distance from basion (mm)	27.66	1.60	26.91	1.02	26.83–28.48	26.35–27.48

Table 2: Hypoglossal canal diameters stratified by morphological shape

Shape	*Max transverse (mm)*	*Max vertical (mm)*	*n (right)*	*n (left)*
Oval horizontal	3.89 ± 0.57	3.28 ± 0.50	8	10
Oval vertical	3.59 ± 0.49	4.07 ± 0.51	6	5
Round	3.45 ± 0.70	3.47 ± 0.55	3	1

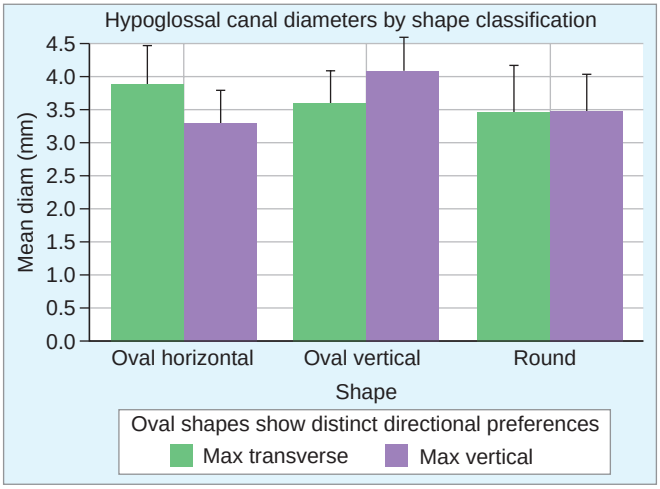

Fig. 3: Comparison of mean transverse and vertical diameters (mean ± SD, mm) across HC shapes: Oval horizontal, oval vertical, and round

support bilateral symmetry in HC dimensions, though individual anatomical variability was observed.

Canal Shape Classification and Distribution

The distribution of canal shapes differed between sides:

Right Side (n = 20 Skulls)

- Oval horizontal: Eight skulls (40%).
- Oval vertical: Six skulls (30%).
- Round: Three skulls (15%).
- Indeterminate: Three skulls (15%).

Left Side (n = 20 Skulls)

- Oval horizontal: 10 skulls (50%).
- Oval vertical: Five skulls (25%).
- Round: One skull (5%).
- Indeterminate: Four skulls (20%).

Mean diameter values according to canal shape are shown in Table 2 and Figure 3, with the corresponding morphological types illustrated in Figure 4.

Anatomical Variability and Anomalies

Notable anatomical variations were identified:

- Absent canal: No cases of an absent HC were observed in the present sample.
- Accessory canal: One skull showed a right-sided accessory canal, another showed a left-sided accessory canal, and a third skull presented bilateral accessory canals, as illustrated in Figures 5 and 6.
- Complete bilateral symmetry: Not all specimens showed bilateral symmetric anatomy; some exhibited asymmetric canal sizes or shapes.

Discussion

Comparative Morphometric Analysis with International Literature

The morphometric dimensions obtained in this Eastern Uttar Pradesh population show several important relationships to published data from other ethnic groups.[1,3–8]

Canal Diameter Comparisons

The mean transverse and vertical diameters observed in this study (3.71 mm transverse right, 3.54 mm transverse left; 3.59 mm vertical right, 3.38 mm vertical left) are notably smaller than those reported in several other populations. Turkish skulls studied by Kizilkanat and colleagues[1] demonstrated intracranial and extracranial diameters of 6.5 ± 1.3 mm and 6.6 ± 1.1 mm, respectively, while Italian population data from Guarna et al.[2] reported external diameters of 6.33 ± 1.40 mm (right) and 6.44 ± 1.59 mm (left). Kumar and colleagues[3] in North Indian populations found mean diameters of approximately 7.48–7.59 mm. Egyptian skulls examined by Farid[4,9] showed intracranial diameters of 6.24 mm (right) and 6.04 mm (left). These differences likely reflect population-specific genetic and developmental factors, emphasizing the importance of ethnicity-specific morphometric baselines for surgical planning.

Canal Length

The distance from the HC intracranial opening to the basion in the present study (27.66 mm right, 26.91 mm left) differs from international standards. Kizilkanat et al.[1] reported HC length of 9.9 ± 1.9 mm, while Guarna et al.[2] measured 8.67 ± 1.86 mm (right) and 8.26 ± 1.67 mm (left), and Berlis and colleagues[8,10] found 7.78 mm. These measurements reflect intracranial extent only, whereas the present study measured the distance to basion (a different landmark), making direct comparison less straightforward but indicating consistent patterns of regional variation.[11]

Canal Shape Predominance

The oval horizontal morphology was most frequently observed (40% right, 50% left), consistent with prior reports. Kizilkanat et al.[1] and earlier studies noted oval horizontal as the predominant configuration, indicating that transverse widening is a common feature across populations despite size differences.[3,5,6]

Bilateral Symmetry

Despite individual asymmetric variations observed in some specimens, the absence of statistically significant right-left differences in this study ($p > 0.05$ for all parameters) aligns with findings from Turkish, Italian, and Indian populations, confirming that bilateral symmetry represents the typical statistical pattern while individual exceptions require preoperative assessment.

Anatomical Variations and Clinical Significance

Accessory Canals and Absent Canals

Accessory HCs were observed in 15% of skulls (3/20: One right-sided, one left-sided, one bilateral), representing rare anatomical variants consistent with anthropological literature. While no absent canals were identified in this Eastern UP sample, Paraskevas et al. documented complete osseous bridging in 19.83% of Greek skulls and Berry and Berry reported double canals in 14.6% of their series, confirming that such variation frequencies demonstrate population-specific patterns.[6,7]

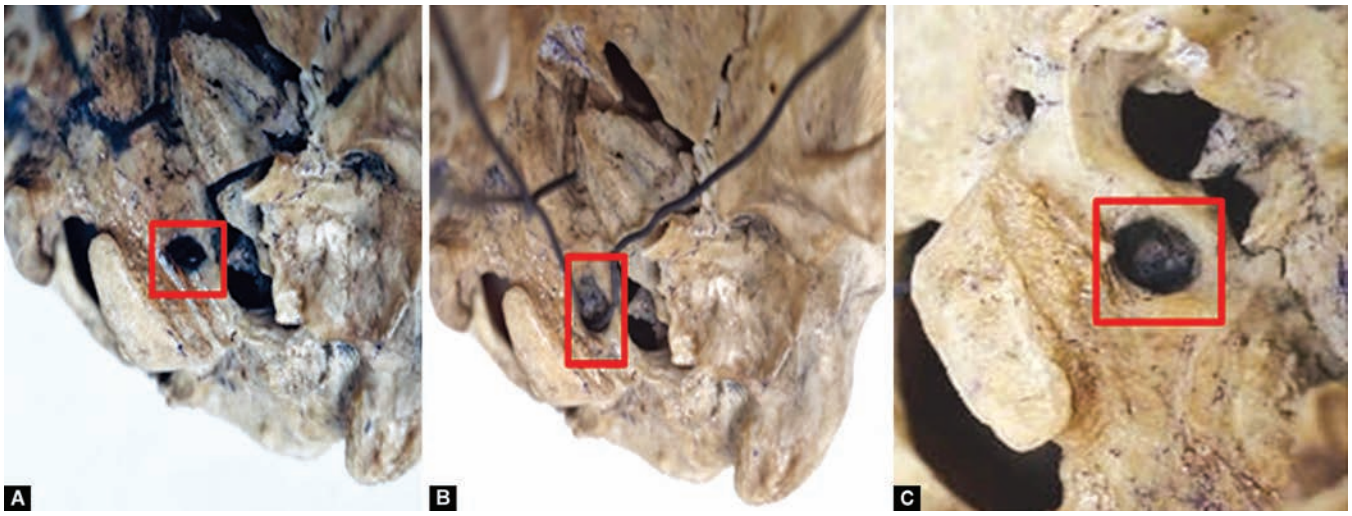

Figs 4A to C: (A) Shows "oval horizontal" shaped HC; (B) Shows "oval vertical" shaped HC; and (C) Shows "round" shaped HC

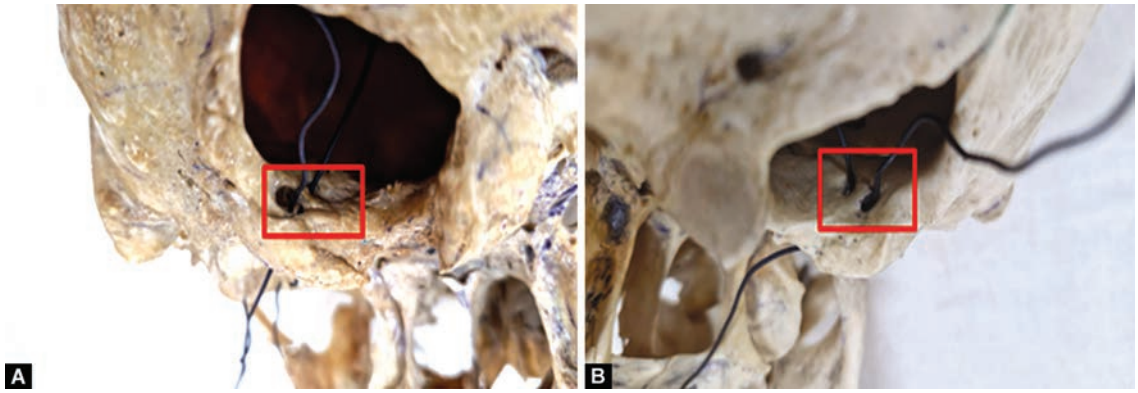

Figs 5A and B: (A) Shows an accessory HC restricted to the right side; (B) Shows an accessory HC only on the left side

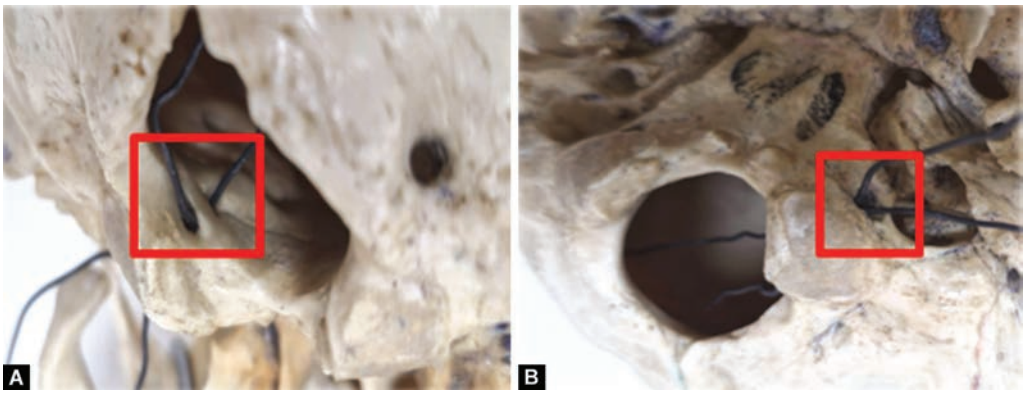

Figs 6A and B: Shows accessory HCs are present on both sides, making it a bilateral variation

Canal Division and Septation

Several classification systems have been proposed for HC variants. Guarna et al.[2] classified canal variations into four types based on septa presence and location (type I: No septum; type II: Bony spine; type III: Incomplete septum; type IV: Complete septum). In their Italian sample, type I (simple canal) occurred in 66%, type IIB in 19%, type IIIB in 2%, and type IVB in 10%. The lower frequency of complete septation in their population contrasted with 43% reported in Polish skulls by earlier researchers.[3,8] In the North Indian population studied by Kumar et al.,[3] bipartite canals were rare, supporting the present observation that complete canal division is less common in Indian populations. Figure 7 illustrates an incomplete bony septum observed within the left HC of one skull specimen.

Fig. 7: Hypoglossal canal showing an incomplete bony septum

Surgical and Clinical Implications

The detailed knowledge of HC anatomy is critical for several reasons:

- Transcondylar approach: During transcondylar surgical resection, the posterior one-third of the OC is typically drilled. Guarna et al.[2] and Kalthur et al.[5] emphasize that the distance from the HC intracranial opening to the posterior margin of the OC is critical (reported as 10.66–12 mm in various populations). Safe drilling zones require this information to avoid neural injury.[5]
- Condyle position relative to HC: Kalthur et al.[5] found that the intracranial opening of the HC was positioned in the middle third of the OC in 100% of specimens (both genders), while the extracranial opening was in the anterior third in 99% (males) and 93.7% (females). This positional consistency provides surgical landmarks.[5]
- Anatomical relationships with adjacent structures: Paraskevas et al.[6] identified associations between double HC variants and posterior condylar canal presence (54% of cases), jugular foramen bridging (42% of cases), and specific OC morphology patterns (eight-shaped type in 52% of double canals). These associations may reflect developmental disturbances in occipital bone ossification.[6]
- Gender differences: Guarna et al.[2] reported that the distance from the inferior edge of the internal HC opening to the inferior margin of the OC differed significantly between males (7.87 ± 1.60 mm) and females (6.76 ± 1.13 mm, $p = 0.011$). This gender-related morphometric difference may be relevant in surgical planning to reduce morbidity and mortality.[2]

Limitations and Clinical Context

The present study was conducted on a limited sample of 20 skulls from a single institution. A larger sample would potentially reveal additional statistical relationships and population-specific patterns. Additionally, the study was performed on dry bone without contemporary neuroradiological findings (CT or MRI), which Guarna et al.[2] noted can provide three-dimensional anatomical information useful for preoperative surgical planning. The classification of some specimens as having an "absent" or "rudimentary" HC requires confirmation with imaging modalities to exclude measurement artifact.

Regional and Population-specific Context

The findings provide baseline data for the Eastern Uttar Pradesh population, with dimensions notably smaller than many international populations but aligned with some North Indian studies.[3] This supports the concept of population-specific morphometric variation that may reflect genetic, developmental, and possibly nutritional factors. For anatomists, neurosurgeons, radiologists, and anthropologists working in this region, these data provide direct reference values superior to applying normative data from geographically or ethnically distant populations.

Conclusion

This morphometric study of the HC in 20 adult skulls from the Eastern Uttar Pradesh region provides detailed dimensional and morphological data including transverse diameters, vertical diameters, distances to bony landmarks, and canal shape classifications. The findings demonstrate bilateral symmetry without statistically significant right-left differences, with oval horizontal morphology as the predominant shape. Comparison with international literature reveals population-specific morphometric variation, with this region's HC dimensions being smaller than many reported populations but consistent with some North Indian and South Indian data. Rare anatomical variants including absent canals and accessory canals were identified, reinforcing the importance of individual anatomical assessment.

The detailed morphometric data presented here, combined with the positional relationships of HC intracranial and extracranial openings to the OC, provide essential information for neurosurgeons planning skull base procedures such as transcondylar approaches. While bilateral symmetry can be generally assumed, preoperative individualized assessment via high-resolution imaging remains essential due to the anatomical variation observed. The data contribute to building a comprehensive anatomical database that accounts for population diversity and supports safer, more precise surgical intervention in the region of the craniovertebral junction and posterior cranial fossa.

Acknowledgments

The authors gratefully acknowledge the financial support provided by the Institute of Eminence (IoE) Scheme, Banaras Hindu University, Varanasi, through its Seed Grant Program.

References

1. Kizilkanat ED, Boyan N, Soames R, et al. Morphometry of the hypoglossal canal, occipital condyle, and foramen magnum. Neurosurg Quart 2006;16(3):121–125. DOI: 10.1097/01.wnq.0000214018.49915.49.
2. Guarna M, Lorenzoni P, Franci D, et al. Hypoglossal canal: An osteological and morphometric study on a collection of dried skulls in an Italian population: Clinical implications. Eur J Med Res 2023;28(1):501. DOI: 10.1186/s40001-023-01489-6.
3. Kumar S, Verma R, Rai AM, et al. Morphological and morphometric analysis of hypoglossal canal in North Indian dry skulls and it's significance in cranial base surgeries. J Clin Diagn Res 2017;11(3):AC08–AC12. DOI: 10.7860/JCDR/2017/24333.9365.
4. Farid SA, Islam O, Abdel Fattah AM. Morphometric study of human adult occipital condyle, hypoglossal canal and foramen magnum in dry skulls of modern Egyptians. Int J Clin Develop Anat 2018;4(1):19–26. DOI: 10.11648/j.ijcda.20180401.13.
5. Kalthur SG, Padmashali S, Bhattarai C, et al. Surgical anatomy of hypoglossal canal for various skull base surgeries. Surg Radiol Anat 2023;45(5):537–543. DOI: 10.1007/s00276-023-03126-7.

6. Paraskevas GK, Tsitsopoulos PP, Papaziogas B, et al. Osseous variations of the hypoglossal canal area. Med Sci Monit 2009;15(3):BR75–BR83. PMID: 19247236.
7. Carolineberry A, Berry RJ. Epigenetic variation in the human cranium. J Anat 1967;101(Pt 2):361–379. PMID: 4227311.
8. Berlis A, Putz R, Schumacher M. Direct and CT measurements of canals and foramina of the skull base. Br J Radiol 1992;65(776):653–661. DOI: 10.1259/0007-1285-65-776-653.
9. Wysocki J, Kobryń H, Bubrowski M, et al. The morphology of the hypoglossal canal and its size in relation to skull capacity in man and other mammal species. Folia Morphol (Warsz) 2004;63(1):11–17. PMID: 15039894.
10. Nuchhi AB, Yatagiri SV, Karjagi SB, et al. Morphological and morphometric analysis of hypoglossal canal and its variations in human dry skulls of North Karnataka Region. Int J Anat Radiol Surg 2019;8(4):AO01–AO04. DOI: 10.7860/IJARS/2019/41992:2507.
11. Yıldız Yılmaz M, Babacan S, Kafa İM, et al. Morphological analysis of the hypoglossal canal and its relationship with surrounding anatomical structures. J Med Dent Inves 2023;4:e230343. DOI: 10.5577/jomdi.e230343.

CASE REPORT

An Unusual Cadaveric Finding of a Floating Gallbladder: Surgical and Diagnostic Implications – A Case Report

Rizwana Farhat[1], Aparna Sharma[2]

Received on: 21 October 2025; *Accepted on:* 13 November 2025; *Published on:* 20 January 2026

Abstract

A floating or wandering gallbladder is a rare anatomical variant in which the organ is entirely enclosed by peritoneum and attached to the liver through a mesenteric fold, giving it a degree of mobility. Normally, the gallbladder is a pear-shaped sac situated within the gallbladder fossa on the visceral surface of the right hepatic lobe. It consists of three distinct regions—the fundus, body, and neck. The fundus is related to the parietal peritoneum of the anterior abdominal wall, while the body and neck lie in close association with the visceral surface of the liver, continuing as the cystic duct. When the gallbladder is suspended by a mesenteric fold, this mobility may predispose it to torsion, a potentially life-threatening surgical emergency.

During a routine dissection session for undergraduate teaching, a rare case of a floating gallbladder was encountered in a male cadaver, where the organ was supported by a peritoneal fold. Although this condition is uncommon, awareness of such variations is essential for laparoscopic surgeons and radiologists to ensure accurate diagnosis and safe surgical planning.

Keywords: Cadaveric dissection, Case report, Cholecystectomy, Floating gallbladder, Gallbladder torsion.

Journal of Anatomical Sciences (2025): 10.5005/jas-11049-0010

Introduction

The extrahepatic biliary apparatus comprises the gallbladder, the right, left, and common hepatic ducts, the cystic duct, and the common bile duct. The gallbladder is typically a pear-shaped reservoir that holds approximately 30–50 mL of bile. It occupies a depression known as the gallbladder fossa on the inferior surface of the right lobe of the liver, adjacent to the quadrate lobe. Structurally, it includes the fundus, body, and neck.

The rounded fundus usually extends slightly beyond the inferior border of the liver and lies opposite the tip of the ninth costal cartilage at the level of the transpyloric plane. The body runs backward and upward toward the porta hepatis, tapering into the neck, which continues as the cystic duct.[1] The peritoneum envelops the fundus and partly covers the body and neck, securing the organ to the visceral surface of the liver. The gallbladder serves to store and concentrate bile until its release into the duodenum during digestion.[2]

Embryologically, abnormal migration of the caudal bud (pars cystica) from the hepatic diverticulum may give rise to positional anomalies of the gallbladder. If the caudal bud advances excessively, it may be embedded within the liver tissue, forming an intrahepatic gallbladder. Conversely, if its migration lags behind the cranial bud (pars hepatica), a free or "floating" gallbladder may result.[3]

Because of the variability in its position and attachments, understanding the detailed anatomy of the gallbladder is essential, particularly during laparoscopic procedures that require careful identification of ducts and vessels.[4] Such anatomical knowledge also aids radiologists in interpreting imaging findings accurately. The present paper reports a cadaveric case of a floating gallbladder and discusses its developmental and clinical implications.

[1,2]Department of Anatomy, Hamdard Institute of Medical Sciences and Research, New Delhi, India

Corresponding Author: Rizwana Farhat, Department of Anatomy, Hamdard Institute of Medical Sciences and Research, New Delhi, India, Phone: +91 8527802126, e-mail: farhat.riz@gmail.com

How to cite this article: Farhat R, Sharma A. An Unusual Cadaveric Finding of a Floating Gallbladder: Surgical and Diagnostic Implications – A Case Report. J Anat Sciences 2025;33(2):64–66.

Source of support: Nil

Conflict of interest: None

Patient consent statement: A written informed consent was obtained from the patient for the publication of details, which can include photographs and/or videos and/or case history to be published in any printed/online journals.

Case Description

During routine cadaveric dissection classes for undergraduate students at the Department of Anatomy, Hamdard Institute of Medical Sciences and Research, New Delhi, the abdomen of a 68-year-old male cadaver (formalin-embalmed) was explored following the guidelines described in Cunningham's Manual of Practical Anatomy, 15th edition. During the dissection, the gallbladder was observed to be free from its usual fossa and completely enveloped by peritoneum, a finding consistent with a floating gallbladder.

The organ appeared morphologically normal, consisting of its fundus, body, and neck. The fundus projected slightly below the inferior surface of the liver (Fig. 1), while the body and neck were

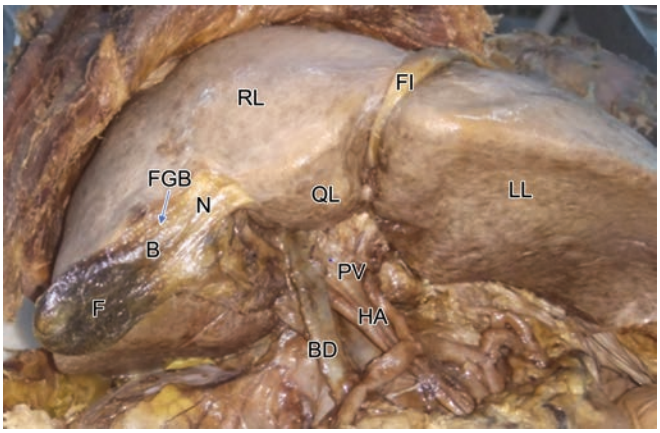

Fig. 1: Floating gallbladder on the inferior surface of right lobe of liver

BD, bile duct; FGB, floating gallbladder (F, fundus; B, body; N, neck); FL, falciform ligament; HA, hepatic artery; LL, left lobe of liver; PV, portal vein; QL, quadrate lobe of liver; RL, right lobe of liver

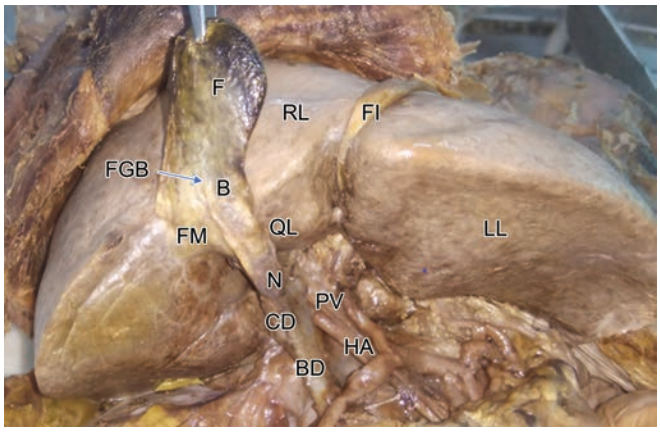

Fig. 2: Floating gallbladder displaced from inferior surface of right lobe of liver

BD, bile duct; CD, cystic duct; FGB, floating gallbladder (F, fundus; B, body; N, neck); FL, falciform ligament; FM, fold of mesentery; HA, hepatic artery; LL, left lobe of liver; PV, portal vein; QL, quadrate lobe of liver; RL, right lobe of liver

aligned along its underside, continuing into the cystic duct (Fig. 2). The gallbladder was attached to the liver by a thin fold of mesentery that permitted partial displacement of its fundus and a segment of the body from the hepatic fossa. This mesenteric connection allowed mobility and could potentially predispose the organ to torsion, leading to acute abdominal symptoms. The gallbladder fossa itself was shallow and poorly defined.

Discussion

A floating gallbladder represents an uncommon anatomical variation in which the organ is completely encased by peritoneum and attached to the liver through a narrow mesenteric fold. This configuration renders the organ unusually mobile, making it susceptible to torsion—a rare but serious cause of acute abdomen that necessitates prompt surgical management.[5]

Several case reports in the literature have documented similar findings. Warfe et al. described a case of gallbladder torsion in a 64-year-old woman following a colonoscopy, likely triggered by mechanical rotation during the procedure.[6] Cho et al. reported a 94-year-old patient who presented with acute right-sided abdominal pain, in whom imaging and subsequent laparoscopic evaluation confirmed torsion of a floating gallbladder.[7] Wu et al. documented a 40-year-old woman with abdominal pain due to a mobile gallbladder, illustrating the variable clinical presentation of this anomaly.[8] Miyakura et al. identified a 61-year-old woman with volvulus of the gallbladder secondary to strangulation by the lesser omentum during laparoscopic surgery.[9] Similarly, Lyons et al. described a 55-year-old female presenting with recurrent epigastric pain, where scintigraphy demonstrated incomplete torsion of a floating gallbladder.[10]

Tarhan, Nicholas, and Atahan independently emphasized two primary predisposing factors for gallbladder torsion: (1) An elongated mesentery that increases its mobility and (2) age-related factors such as visceroptosis and weakening of connective tissue that allow the organ to hang freely within the peritoneal cavity, increasing torsion risk.[5,11,12]

Sreekanth identified two instances of floating gallbladder among 45 formalin-preserved liver specimens – one in which the organ was displaced downward by a mesenteric fold, and another where it was completely intraperitoneal.[3] Similarly, Setty and Katikireddi reported a floating gallbladder in a 50-year-old male cadaver suspended by a peritoneal fold, closely resembling the findings in the present report.[13]

Conclusion

Although variations in the anatomy of the gallbladder are rare, they carry significant importance for both radiologists and surgeons, particularly in laparoscopic procedures. The presence of a mesenteric fold that suspends the gallbladder increases its mobility and predisposes it to torsion and other complications, such as acute cholecystitis and abdominal pain. Awareness of these variations helps clinicians avoid diagnostic errors and intraoperative complications. Detailed anatomical knowledge thus plays a vital role in improving surgical outcomes and minimizing patient morbidity and mortality.

Orcid

Rizwana Farhat https://orcid.org/0000-0002-9406-3146

References

1. Sinnatamby CS. Last's anatomy: Regional and applied. 12th ed. London (UK): Churchill Livingstone; 2011. pp. 264–265.
2. Snell RS. Clinical anatomy. 9th ed. Philadelphia (USA): Lippincott Williams & Wilkins; 1995. p. 199.
3. Sreekanth T. Incidence of floating/wandering gallbladders: A cadaveric study and its clinical implications. Int J Anat Res 2017;5(1):3338–3341. DOI: 10.16965/ijar.2016.470.
4. Nadeem G. A study of the clinico-anatomical variations in the shape and size of the gallbladder. J Morphol Sci 2016;33(2):62–67. DOI: 10.4322/jms.082714.
5. Tarhan OR, Barut I, Dinelek H, et al. Gallbladder volvulus: Review of the literature and case report. Turk J Gastroenterol 2006;17(3):209–211. PMID: 16941256.
6. Warfe SR, Dobson H, Hong MKH. Torsion of wandering gallbladder following colonoscopy. J Med Case Rep 2013;808751. DOI: 10.1155/2013/808751.

7. Cho YP, Kim HJ, Jung SM, et al. Torsion of the gallbladder: Report of a case. Yonsei Med J 2005;46(6):862–865. DOI: 10.3349/ymj.2005.46.6.862.
8. Wu WC, Chau GY, Suae CW, et al. Wandering abdominal pain due to a floating gallbladder. Dig Liver Dis 2013;45:e13. DOI: 10.1016/j.dld.2013.05.003.
9. Miyakura Y, Ohta ASM, Lefor AT, et al. Floating gallbladder strangulation. Surg Today 2012;42(7):693–696. DOI: 10.1007/s00595-012-0171-3.
10. Lyons KP, Challa S, Abrahm D, et al. Floating gallbladder: A prelude to torsion—A case report. Clin Nucl Med 2000;25(3):182–183. DOI: 10.1097/00003072-200003000-00004.
11. Nicholas JM. Image of the month: Gallbladder volvulus. Arch Surg 2002;137. DOI: 10.1001/archsurg.137.6.741.
12. Atahan K, Gur S, Tarcan E, et al. Torsion of the gallbladder. Turk J Gastroenterol 2007;18(2):129–130. PMID: 17602365.
13. Setty SNRS, Katikireddi RS. Cadaveric floating gallbladder and its clinical significance: A case report. Int J Curr Res Rev 2013;5(23):53–54.

BRIEF RESEARCH COMMUNICATION

Study of the Usage of Multimedia in Medical Education by Medical Teachers

Vinay Sharma[1], CS Ramesh Babu[2]

Received on: 26 November 2025; *Accepted on:* 07 January 2026; *Published on:* 20 January 2026

Abstract

Introduction: Selection of teaching tools in medical education may depend upon subject—like anatomy that majorly depends upon diagrams, age factor, or training of faculty members in newer teaching tools.

This study investigated the factors influencing the adoption of multimedia in medical education by medical teachers in two colleges in Western Uttar Pradesh. The aim was to identify factors affecting the selection of teaching-learning mediums and multimedia use among medical faculties.

Research and methodology: A cross-sectional study was conducted using a 12-questionnaire administered to 140 faculty members (assistant professor and above). Data was analyzed using Excel, Chi-square tests, and presented in tables and diagrams.

Results: Results revealed that 69% of faculty favored multimedia or a combination of conventional and multimedia methods, while 31% preferred conventional methods (chalk and board or walk and talk). While age-group (30–50 vs 51–70) showed no statistically significant difference in multimedia use ($p > 0.05$), trained faculty significantly preferred multimedia more than nontrained faculty ($p < 0.0001$). No significant difference was found between pre/paraclinical and clinical subjects regarding multimedia usage ($p > 0.05$). The most used teaching medium was PowerPoint (PPT), followed by chalk and board.

Keywords: Chalk and board, Conventional method of teaching, Medical education, Multimedia, Teaching tools.

Journal of Anatomical Sciences (2025): 10.5005/jas-11049-0014

Introduction

The conventional method of teaching, that is, lecture and walk and talk in real time, has been in the curriculum since time immemorial. Multimedia use for teaching medical students is increasing in the present scenario.[1]

Yet the use of multimedia and audiovisual aids is increasing day by day, somewhat also replacing a few of the conventional methods of teaching, but still a group of medical faculties favors the conventional teaching due to adjustments of the speed, hand-drawn diagrams, subject support, or age factor, etc. Sabitha Vadakedath stated that many medical faculties in the advanced phase of their teaching career find difficulty to opt for multimedia-based methods of teaching.[2]

On the contrary, many of the faculty members accept multimedia for medical education, larger curriculum coverage in a limited time, shortage of faculty members, handwriting issues, etc.

Many have proven that multimedia is more impactful, learner-oriented, and effective in comparison with conventional methods of teaching (chalk and board or walk and talk).[3–5] So knowing the factors that are affecting the selection of one of them can help to understand how the use of multimedia can be increased and can be imposed effectively in medical education may be helpful.

This may be the only factor; other factors affecting the selection of teaching–learning medium are also a matter of research.

Aim

To find factors affecting the use of multimedia by medical faculty in teaching.

[1,2]Department of Anatomy, Muzaffarnagar Medical College, Muzaffarnagar, Uttar Pradesh, India

Corresponding Author: Vinay Sharma, Department of Anatomy, Muzaffarnagar Medical College, Muzaffarnagar, Uttar Pradesh, India, Phone: +91 9837154651, e-mail: vinay_sharma1979@yahoo.com

How to cite this article: Sharma V, Babu CSR. Study of the Usage of Multimedia in Medical Education by Medical Teachers. J Anat Sciences 2025;33(2):67–69.

Source of support: Nil

Conflict of interest: None

Objectives

- To find out the factors affecting the selection of the teaching–learning medium.
- To find out what the factors are that affect the use of multimedia teaching in medical faculties.

Research and Methodology

This cross-sectional study was conducted in two medical colleges of western Uttar Pradesh. The project was approved by the ethical committee and the Dean, and written informed consent from the faculty was taken. A preformed questionnaire (12 questions) was given to 150 faculty members (assistant professors and above) personally and collected up to 29/02/2020. The questionnaire was validated by faculty members of Muzaffarnagar Medical College and NHL MMC, Ahmedabad. A total of 10 faculty members, who

Table 1: Showing the distribution of usage of multimedia in two different age-groups: 30–50 and 51–70 years

Age-group	*Conventional method of teaching*	*Multimedia use for teaching*	*Total*
51–70	10	18	28
30–50	50	62	112
Total	60	80	$N = 140$
Chi-square test	$\chi^2 = 0.05$, $\lambda = 0.729$	$p > 0.05$	Not significant

Table 2: Showing the distribution of usage of multimedia in two different groups: Trained and not trained

Subject	*Trained (n = 72)*	*Nontrained (n = 68)*	*Total*
Using multimedia	56	14	70
Not using multimedia	16	54	70
Total	72	68	$N = 140$
$\chi^2 = 0.05$,	$\lambda = 45.75$	$p < 0.0001$	Highly significant

Table 3: Showing the distribution of usage of multimedia in two different groups of faculty members (pre/paraclinical departments)

Subject	*Pre/Paraclinical departments (82)*	*Clinical departments*	*Total*
Using multimedia	47	36	83
Not using multimedia	23	34	57
Total	70	70	$N = 140$
$\chi^2 = 0.05$	$\lambda = 3.58$	$p > 0.05$	Not significant

submitted questionnaires after29/02/2020, were not included in the study. The questionnaire was collected, and data were arranged in an Excel sheet and analyzed with the help of Excel formulas and the Chi-square test, and tables and diagrams were prepared.

Results

- A total of 31% faculty favor the use of the conventional (chalk and board or walk and talk) method for teaching–learning sessions.
- The remaining 69% favor either multimedia usage or both.
- There was no statistically significant difference between age-groups 30–50 and 51–70 ($p > 0.05$) (Table 1).
- Trained faculty prefer multimedia more in teaching ($p < 0.0001$) (Table 2).
- There was no statistically significant difference between pre/paraclinical subjects and clinical subjects in using multimedia ($p > 0.05$) (Table 3).
- The teaching–learning medium used most is PPT, followed by the chalk and board.

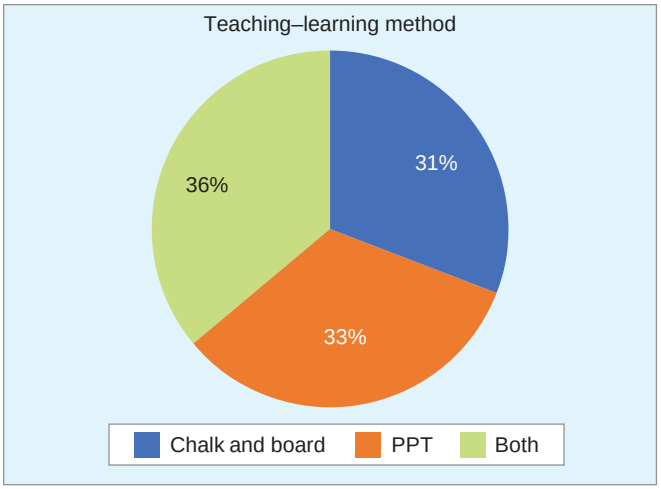

Fig. 1: Pie chart showing the uses of multimedia by faculty members

Discussion

Multimedia is a combination of more than one media type, such as text (alphabetic or numeric), symbols, images, pictures, audio, video, and animations, usually with the aid of technology for the purpose of enhancing understanding or memorization.[6] In the present time, especially after the COVID pandemic, medical education has shifted its dependency more and more toward the use of multimedia (smart boards, Google Classroom, videos, and AI), in order to maintain high-quality medical education, administrators, and educators are forced to look for modern technologies and uses of multimedia.[7] Uses of multimedia and modern technologies are preferred by some medical educators and sometimes criticized for their fast speed, not compatible with all, requiring modern instruments and proper training, and particularly by subjects.

The less usage of multimedia during medical teaching by elder faculty members, as concluded by some authors, may be due to a lack of interest in training.[2]

This study was designed for evaluating what percentage of faculty members using multimedia willingly and what are the factors impacting the use of multimedia during their moderation (Fig. 1).

Percentages of multimedia-using faculty were 69% comparatively a little less than 83.09% of faculty members using the computers for conducting the sessions, as observed in the study of Agrawal and Kumari.[8] But one of the findings of this research was that "most users belong to the younger age-group, while most nonusers are of the older age" did not coincide with the present study, as in our results, there was no statistically significant difference between age-groups 30–50 and 51–70 ($p > 0.05$). This may be due to group division or due to the increasing frequency of training in the present scenario. One comment of Satish C. Agrawal and Anita Kumari was significant, that out of these 12.67 percent of nonusers of the computers, the reasons were either not feeling the need for computers or an inability to learn.

Factors like department or sex or any other factors were not significantly impacting the use of multimedia in medical education, similar to other studies.[7,8]

The present study draws the opinion which was the impact of the age does not affect the use of multimedia in medical education, as we divided two groups of medical educators into 30–50 years and 51–70 years and compared and found that there was no statistically significant difference between the age-group 30–50 and 51–70 ($p > 0.05$). This finding is opposite to the opinion of studies that concluded most of the senior faculty lacked adequate knowledge of newer computer-related teaching aids and showed a preference for older methods.[9]

The difference in this outcome of the present study may be due to the increasing essentiality of training of multimedia in medical faculty or due to the lesser average age in the studied group in other studies.

The direct or indirect impact of the training is one of the most important factors affecting the use of multimedia in medical education.

Training provides a better teaching tool for moderating the session in which a medical faculty is trained.

Conclusion

The impact of multimedia use in medical education is observed by many researchers, but factors affecting the use of multimedia by medical teachers still need to be analyzed. The present study concludes that training of medical faculty members is a definitive factor affecting the use of multimedia in medical education, and by hands-on training of different multimedia tools, we can increase the use and impact of multimedia in medical education.

Acknowledgments

The authors would like to highly thankful to my mentor for this ACME project 1. Dr Kanan Shah Mam Department of Anatomy at NHL Municipal Medical College, Ahmedabad. 2. Santosh Kumar Raghav (AP/statistician) Department of Community Medicine, Muzaffarnagar Medical College, Muzaffarnagar.

Disclaimer

This article is part of this ACME project completed at the NHL Municipal Medical College, Ahmedabad.

Orcid

Vinay Sharma https://orcid.org/0009-0008-5590-9808
CS Ramesh Babu https://orcid.org/0000-0002-6505-2296

References

1. Sharma AK, Sharma HR, Choudhary U. E-Learning versus traditional teaching in medical education: A comparative study. JK Sci 2020;22(3):137–140.
2. Vadakedath S, Sudhakar T, Kandi V. Assessment of conventional teaching technique in the era of medical education technology: A study of biochemistry learning process among first year medical students using traditional chalk and board teaching. Am J Educ Res 2018;11(8):e5396. DOI: 10.7759/cureus.5396.
3. Welch MC, Yu J, Larkin MB, et al. A multimedia educational module for teaching early medical neuroanatomy. MedEdPORTAL 2020;16. DOI: 10.15766/mep_2374-8265.10885.
4. Jahanpour, Paymard A, Pouladi S, et al. Comparing the durability of professional ethics' learning in two methods of group discussion and multimedia software. Res J Med Sci 2016;10(3):120–123. DOI: 10.17795/nmsjournal26920.
5. Fani MM, Mehravar S, Mehrabi M. Level of learning and satisfaction through traditional methods and the use of multimedia: A comparative study. Media 2014;5(7):72–78.
6. Guan N, Song J, Li D. On the advantages of computer multimedia-aided English teaching. Procedia Comput Sci 2018;131:727–732. DOI: 10.1016/j.procs.2018.04.317.
7. Tabatabai S. COVID-19 impact and virtual medical education. J Adv Med Educ Prof 2020;8(3):140–143. DOI: 10.30476/jamp.2020.86070.1213.
8. Agrawal SC, Kumari A. Use of the computer and internet by teachers in medical education: A study at a medical college of North India. South East Asian J Med Educ 2013;7(2):40–44. DOI: 10.4038/seajme.v7i2.139.
9. Rajkumari B. Barriers in using computer related teaching aids among faculty members in a newly established medical college: A cross sectional study. Int J Med Public Health 2016;6(4):170–174.